HI in the Magellanic Clouds, Looking Back and Looking Ahead

John Dickey
University of Tasmania
10 September 2018

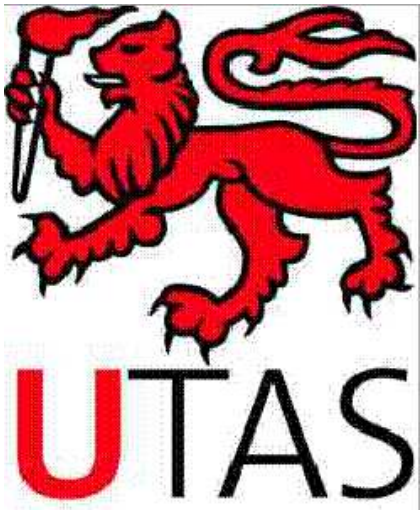

The Four Eras in Magellanic HI:

- 1954-1970 The Hindman Era at Potts Hill
- 1970-1984 The Matthewson Era at Parkes
- 1995 – 2005 The Staveley-Smith Era at the ATCA (data includes ATCA + Parkes)
- The McClure-Griffiths et al.[1] Era at ASKAP (plus data from Parkes + ATCA precursors)

[1] Helga Denes, Katie Jameson, Enrico Di Teodoro, Buckland-Willis, James Dempsey, Nick Pingel, Snezana Stanimirovic, Liu Boyang, Lister Staveley-Smith,, JD.

Kerr, Hindman, and Robinson 1954

1948 pioneers:
Ruby Payne-Scott
Alec Little
Wilbur Christiansen

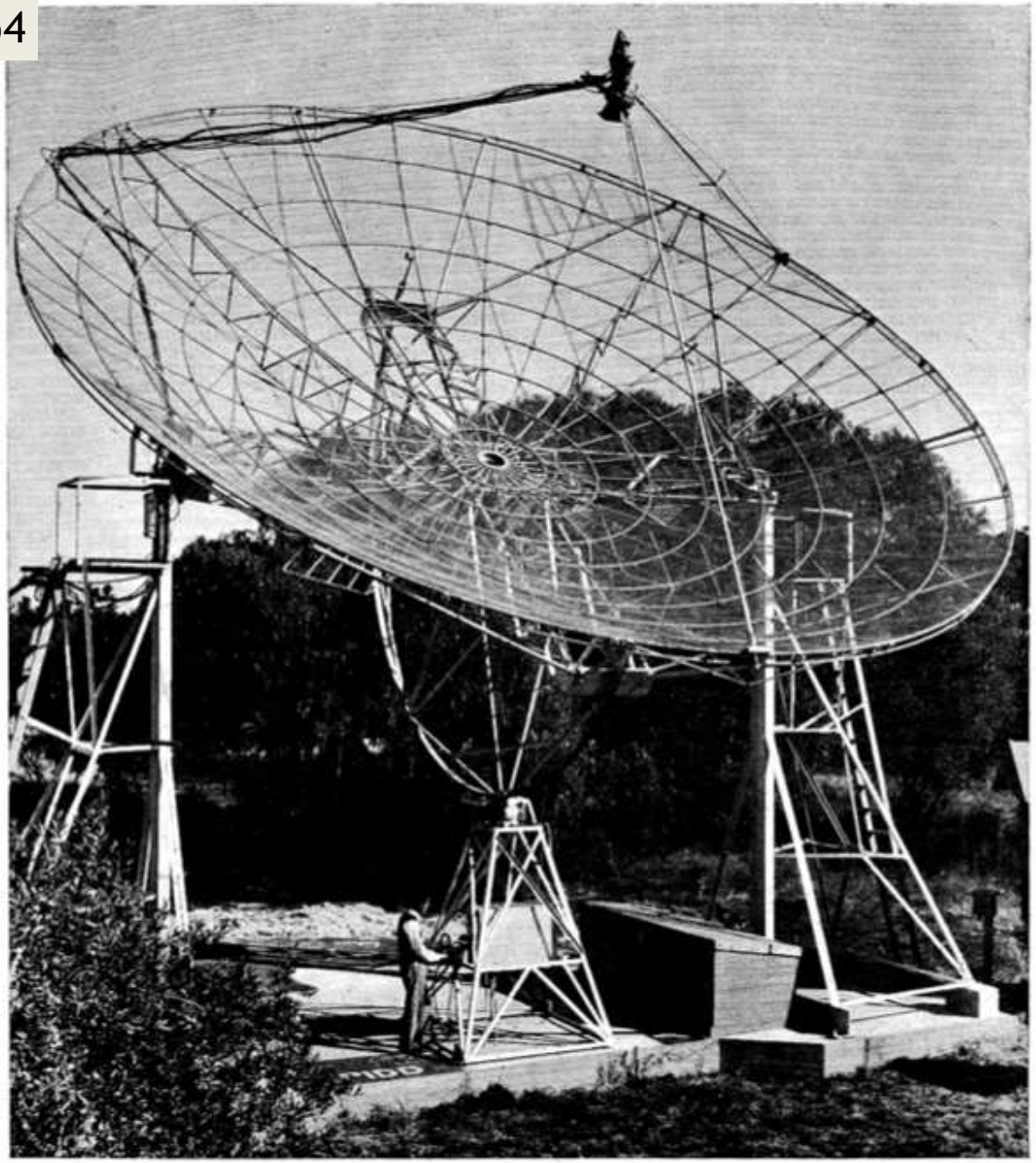

The 36-ft. paraboloid at Potts Hill, near Sydney.
The aerial is mounted as a transit instrument.

Kerr, Hindman, and Robinson 1954

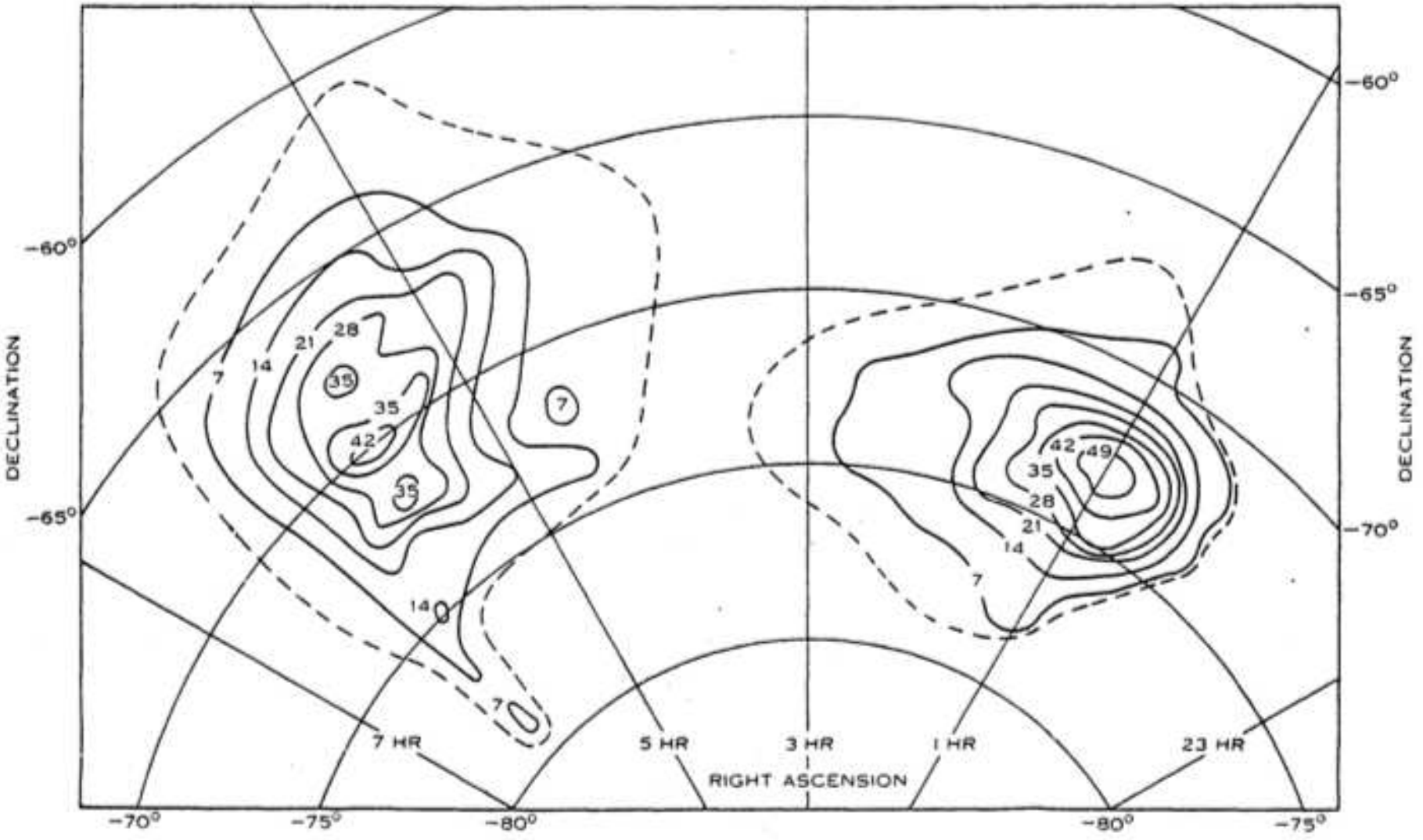

Fig. 1.—Contours of integrated brightness. (Unit = 10^{-16} W m^{-2} sterad^{-1}.) The dashed line approximately encloses the areas within which radiation was detected.

Hindman, Kerr, and McGee 1964

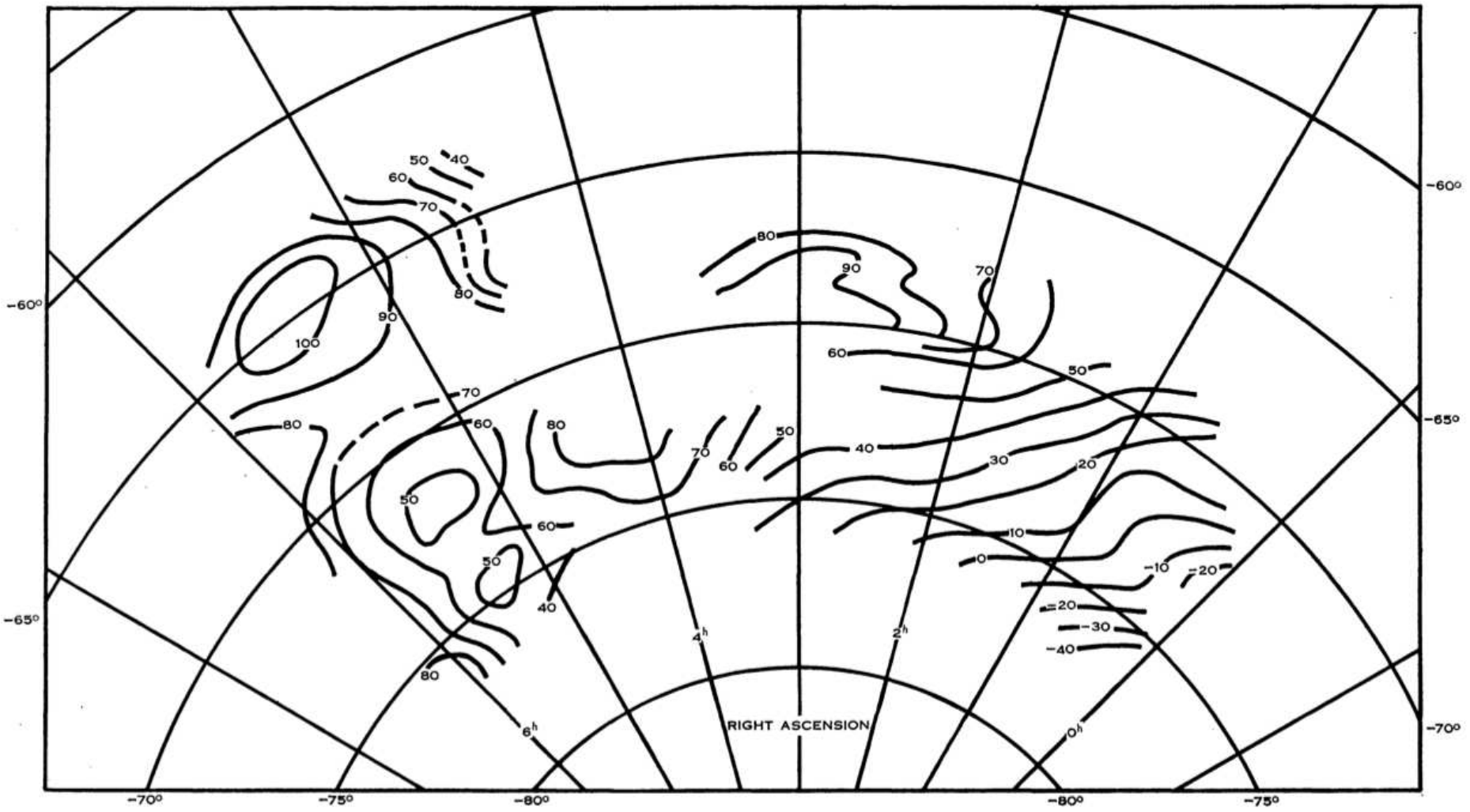

Fig. 7.—Contours of median radial velocity of neutral hydrogen profiles in the Magellanic System, referred to the galactic centre. Contour interval 10 km/s.

Results from Potts Hill:

- HI mass LMC: 6×10^8 M_o SMC: 4×10^8 M_o

Modern value (Bruns et al 2005 A&A 432, 45): 4.4×10^8 $[d/50kpc]^2$ and 4.0×10^8 $[d/60kpc]^2$ plus 4.9×10^8 $[d/55kpc]^2$ for the Bridge, Stream, Leading Arm etc.

- Sizes much larger than the optical

(1) a rotational pattern in the Large Cloud,

(2) a general gradient across the whole composite object,

(3) a possible, but much less definite, rotation effect in the Small Cloud.

- M_{tot} LMC = 0.7 to 1 x 10^{10} M_o
  SMC = ???

LMC (van der Marel and Kallivayalil 2014) : 1.7×10^{10} $[d/50kpc]^2$ inside R=8.7 kpc
SMC (de Teodoro et al 2018 in prep): 2.4×10^9 $[\sin(51^o)/\sin(i)]$

The Parkes Decades (1964-1984):

McGee and Milton 1966

Parkes view of HI in the LMC

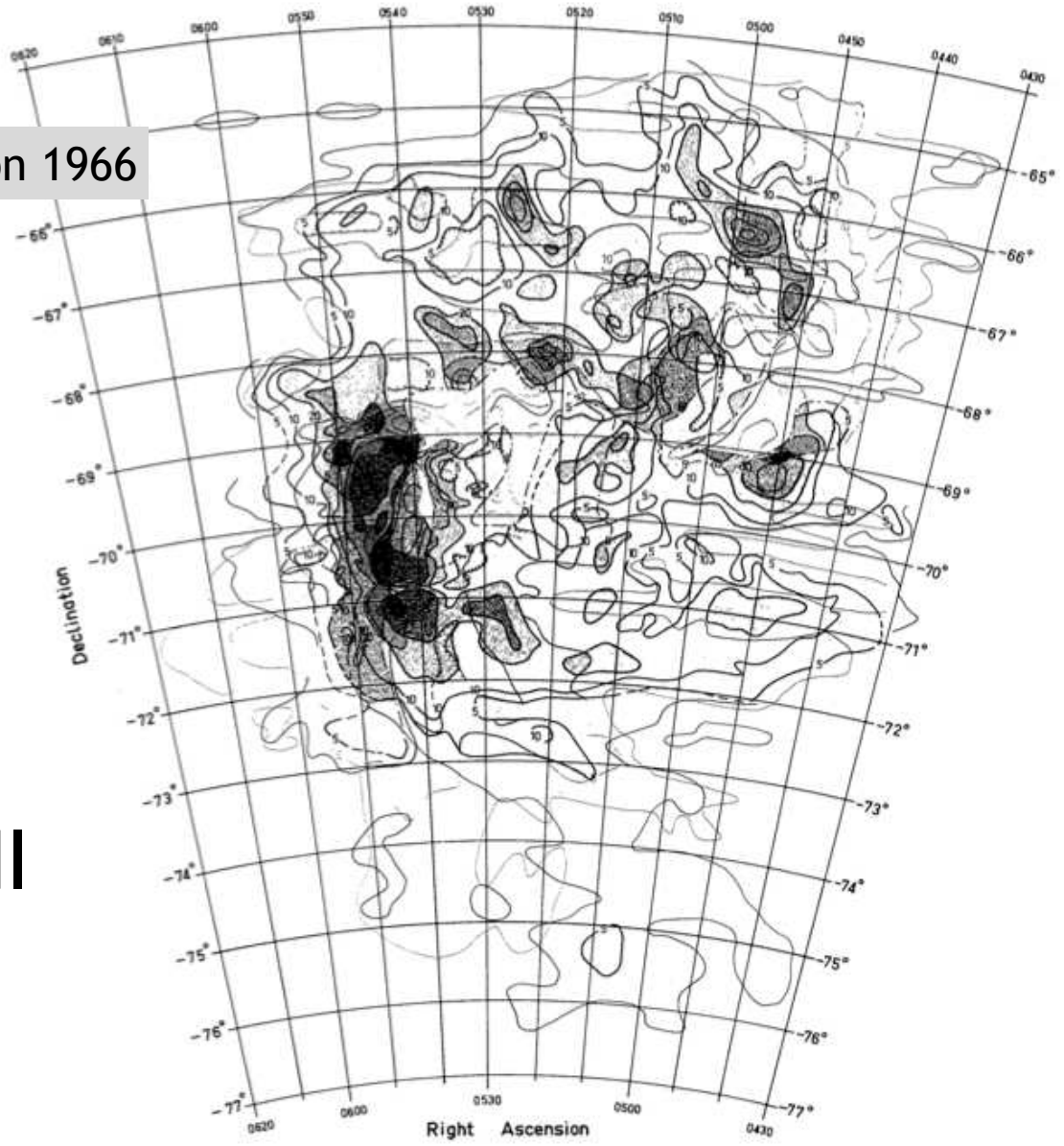

Fig. 5.—Composite distribution of neutral hydrogen in the Large Magellanic Cloud in terms of H-line peak intensities T_{max}. *Red*: gas near +300 km/sec; *orange*: gas near +273 km/sec; *blue*: gas near +243 km/sec.

Hindman 1967

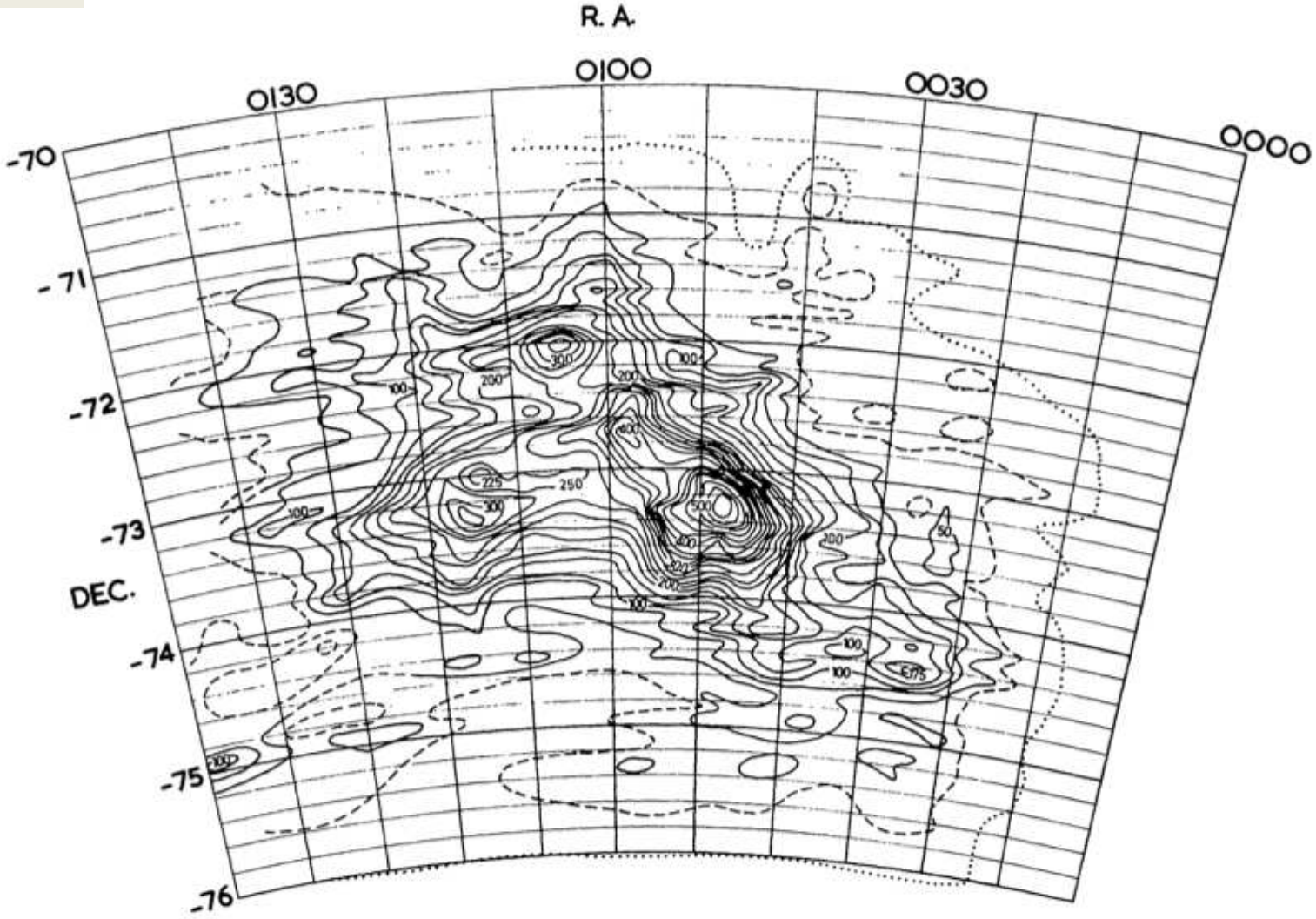

Fig. 2.—Contours of 21 cm H-line integrated brightness over the area of the SMC (contour unit = $3 \cdot 5 \times 10^{-17}$ W m^{-2} sr^{-1}). The outer (dotted) contour is an estimate of the limits of detectable radiation with the present receiver sensitivity. Epoch of coordinates 1975.

Mathewson and Ford 1984

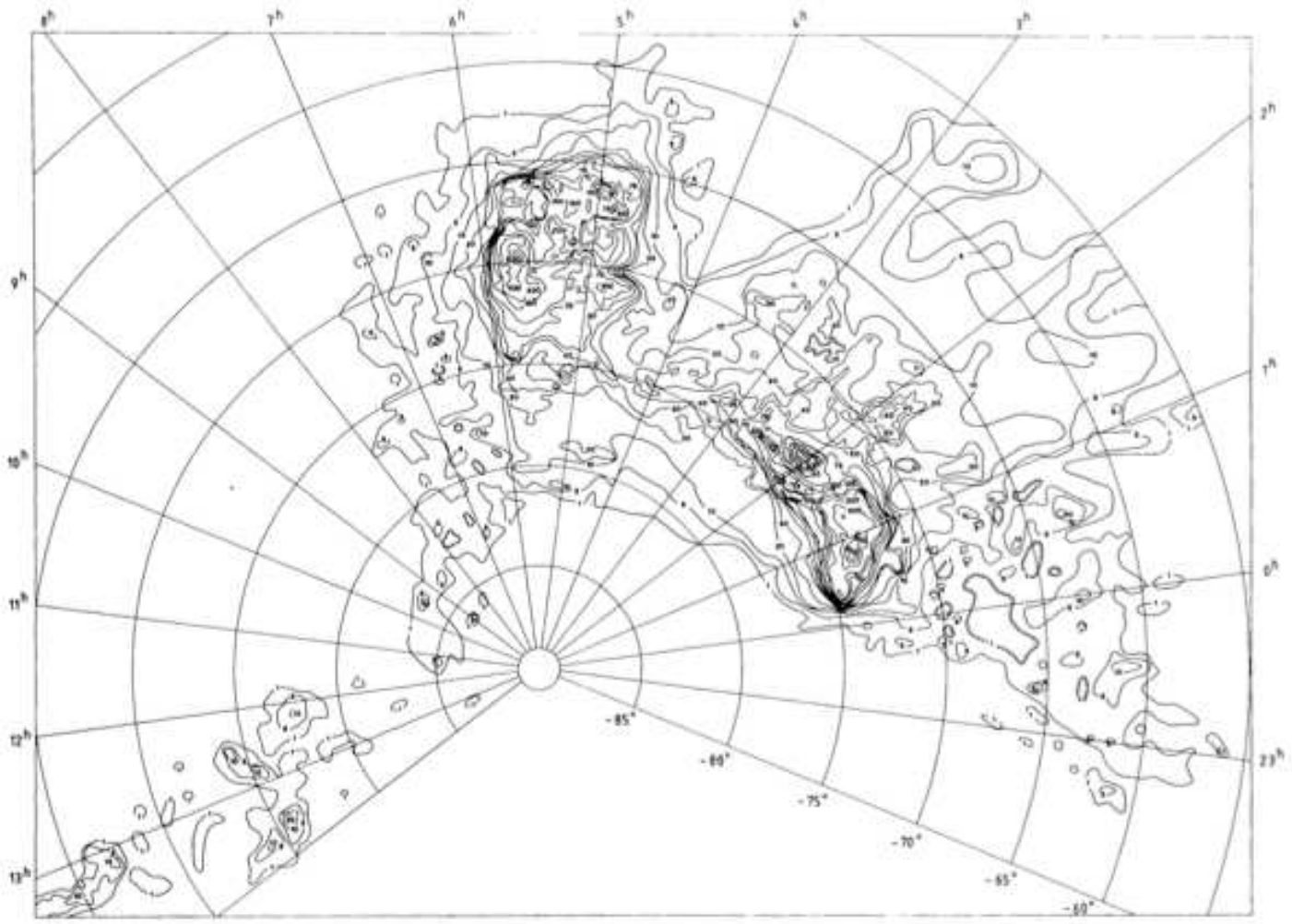

Fig. 2 The integrated HI surface density contours of the region of the LMC and SMC obtained with the 64-m Parkes radiotelescope. The contour unit is 10^{19} atoms cm^{-2}. Data have been taken from Mathewson et al. (1979), Mathewson, Ford and Fisher (1983), McGee and Milton (1966), and Hindman (1967).

The Mosaic + Multibeam Era:

1995 – 2005

Staveley-Smith, Kim, Stanimirovic, Mueller, Matthews, For

Sault, Kileen

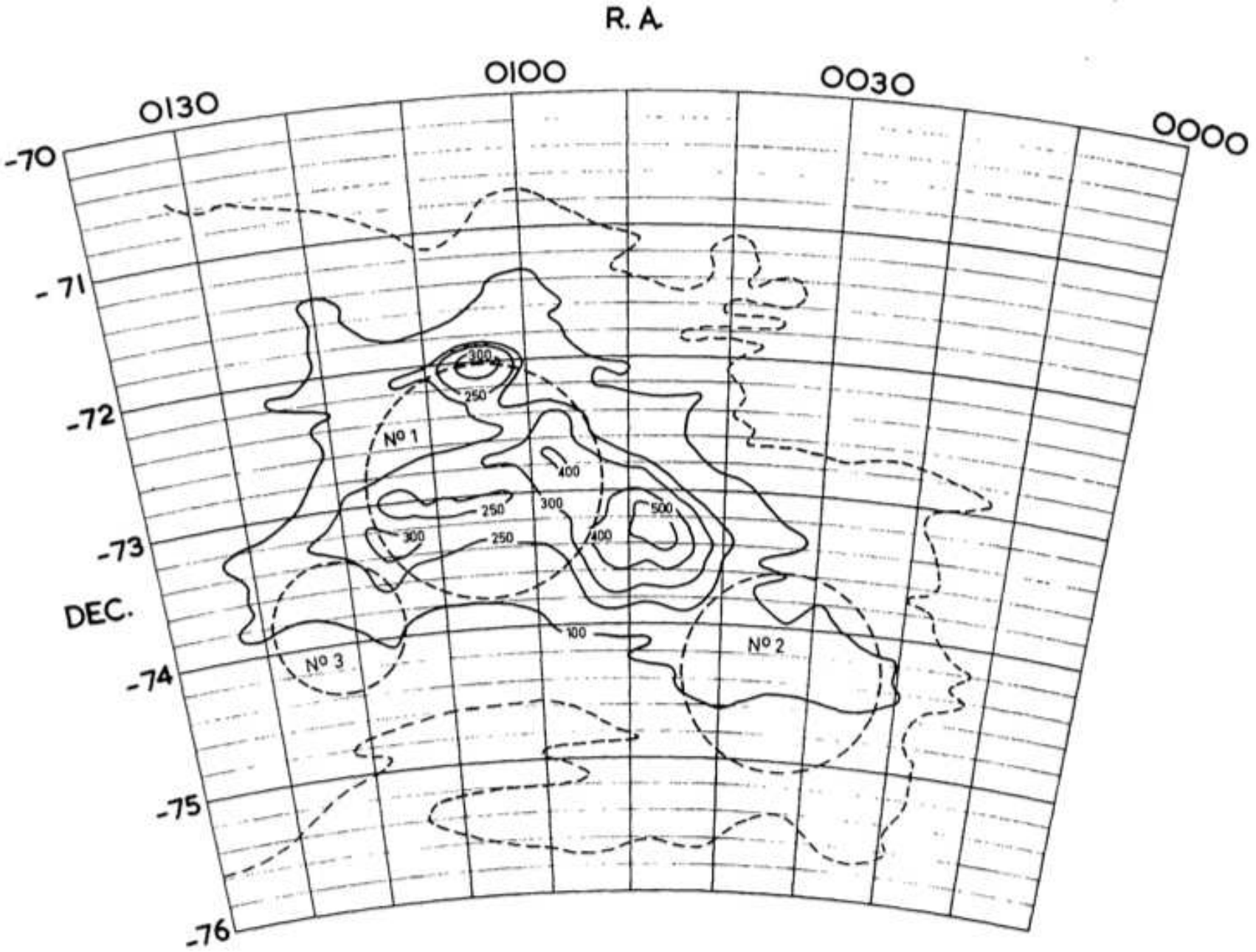

Fig. 11.—Contours of integrated brightness with the positions of three expanding shells of gas indicated (dashed circles).

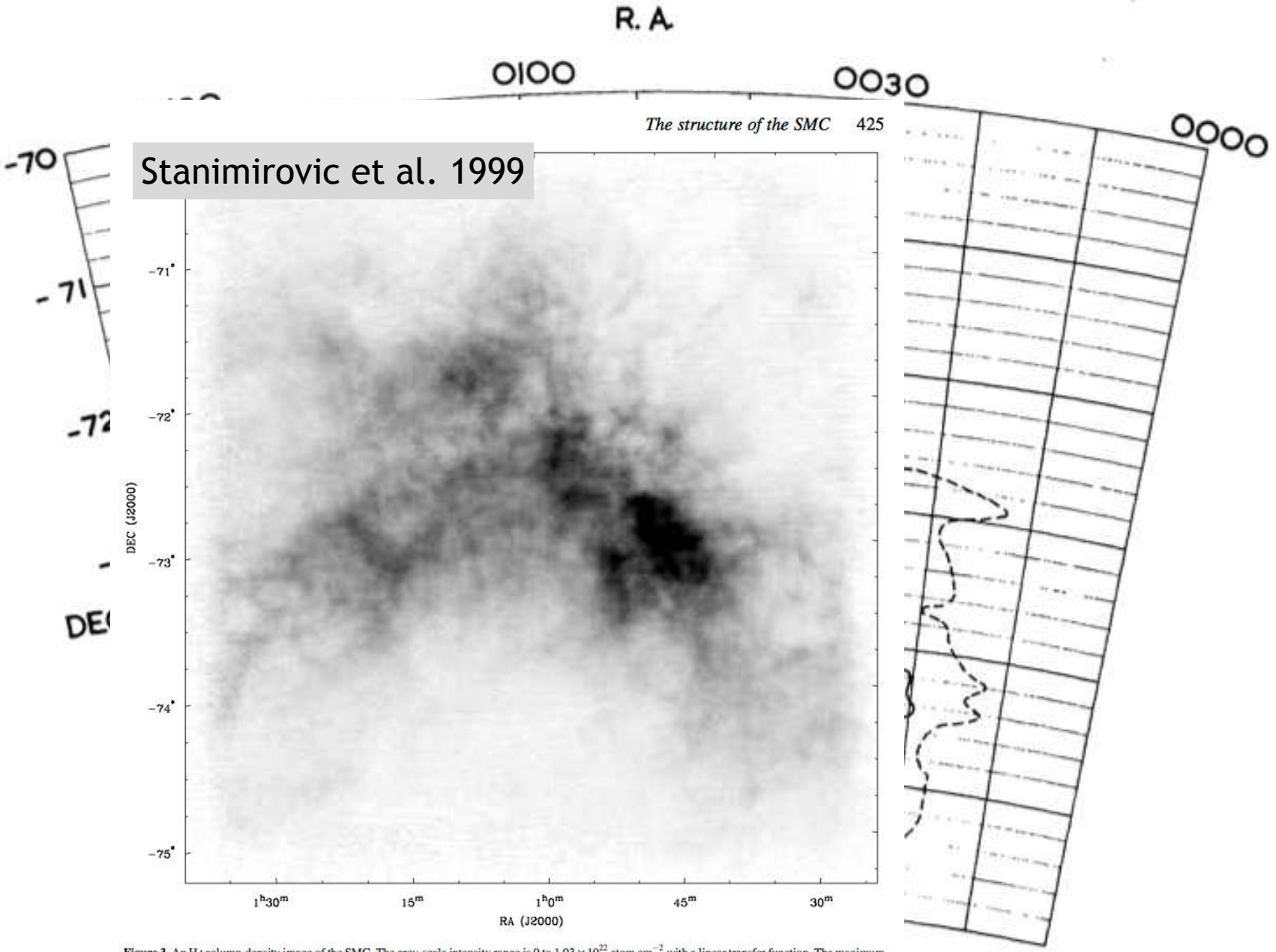

Figure 3. An H I column-density image of the SMC. The grey-scale intensity range is 0 to 1.03×10^{22} atom cm^{-2} with a linear transfer function. The maximum H I column density, 1.43×10^{22} atom cm^{-2}, is at position RA $00^h47^m33^s$, Dec $-73°05'26''$ (J2000).

Fig. 11.—Contours of integrated brightness with the positions of three expanding shells of gas indicated (dashed circles).

Stanimirovic et al. 2000

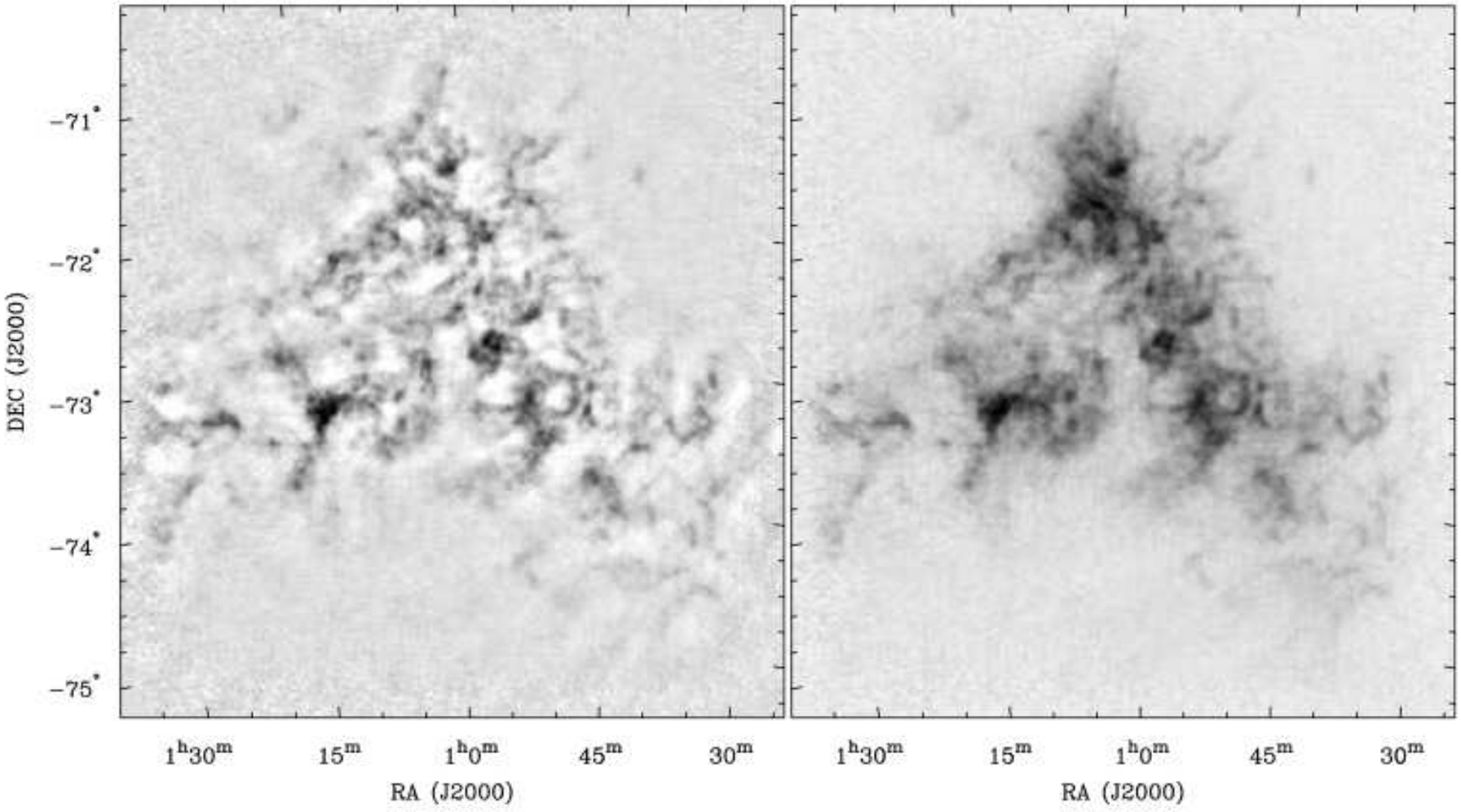

Figure 1. An H I image of the SMC at heliocentric velocity 169 km s^{-1} before (left) and after (right) adding the Parkes short-spacing data. The grey-scale intensity range is −11 to 87 K and −11 to 126 K, respectively. The FWHM beam size is 98 arcsec.


The Australian Square Kilometre Array Pathfinder -- ASKAP

Mk I (BETA) 2011

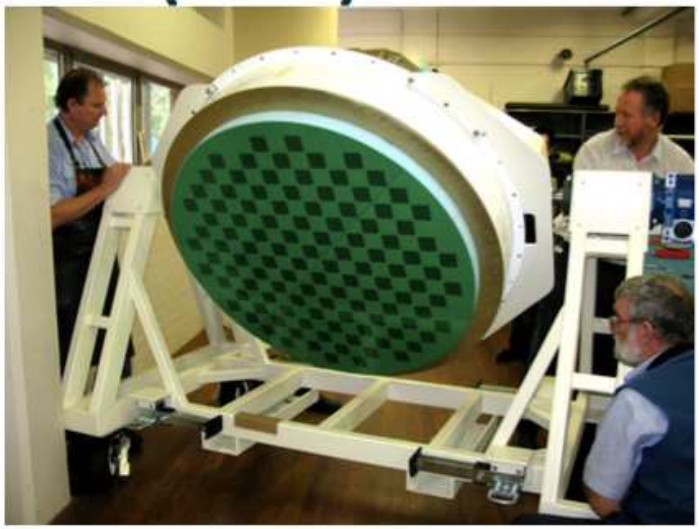

Schinckel et al., APMC 2011
Hotan et al., PASA 2014

PAF slides from Schinckel, Chippendale, Hotan, Voronkov, McConnell

Mk II (ASKAP) 2014

Hampson et al., ICEAA 2012

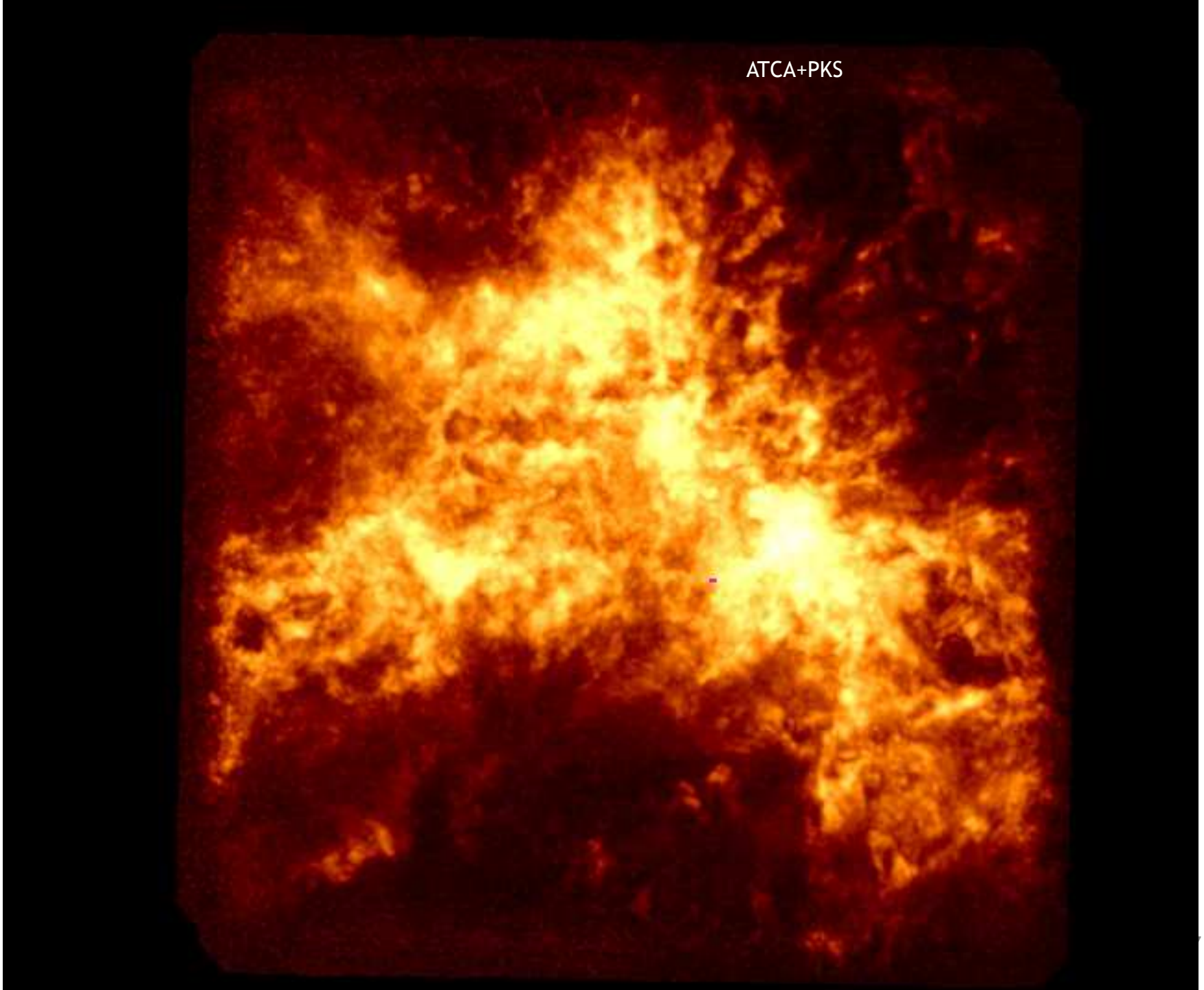
ATCA+PKS


ASKAP+Parkes
16 Antennas
McClure-Griffiths et al

Anomalous external features

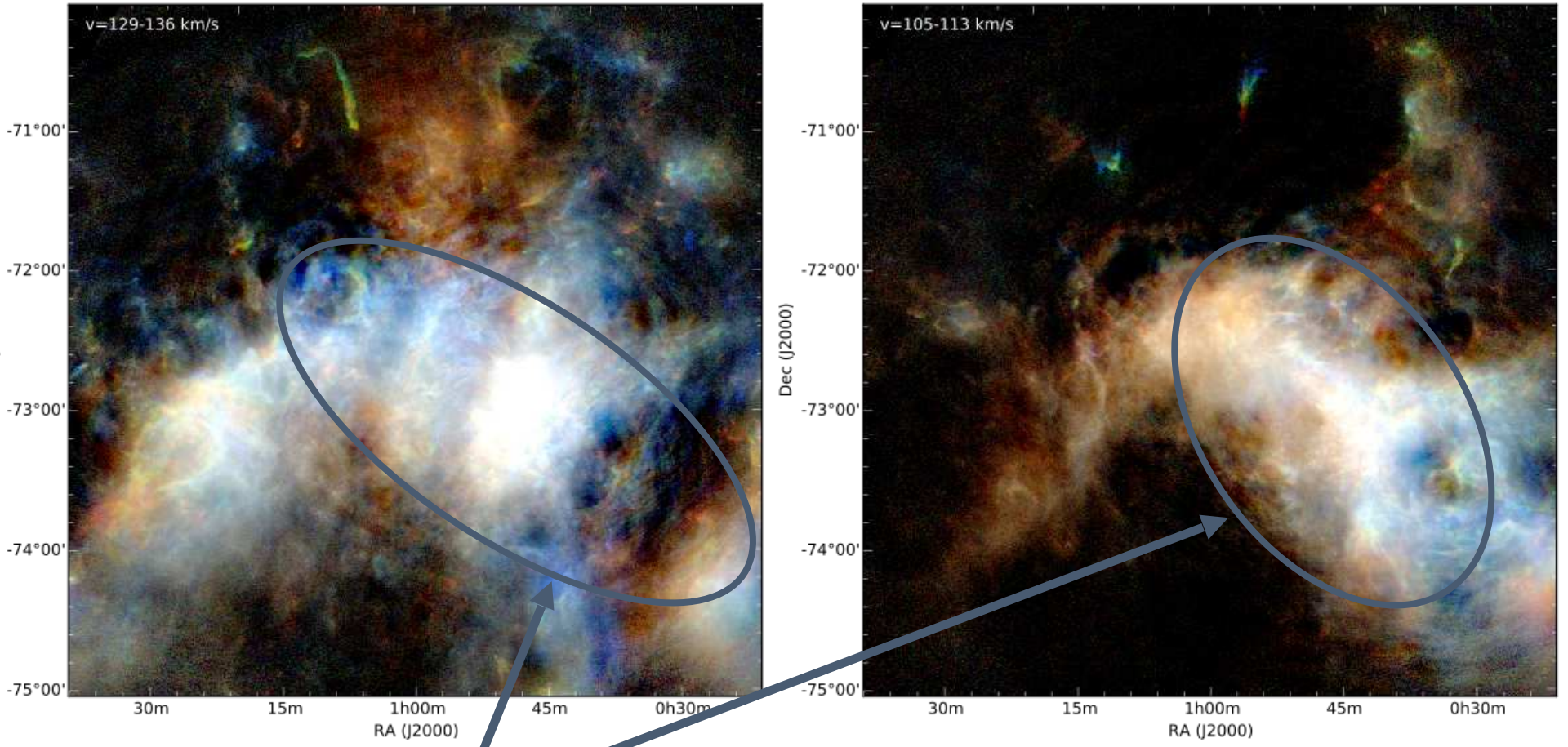

"Normally" rotating gas

Anomalous external features

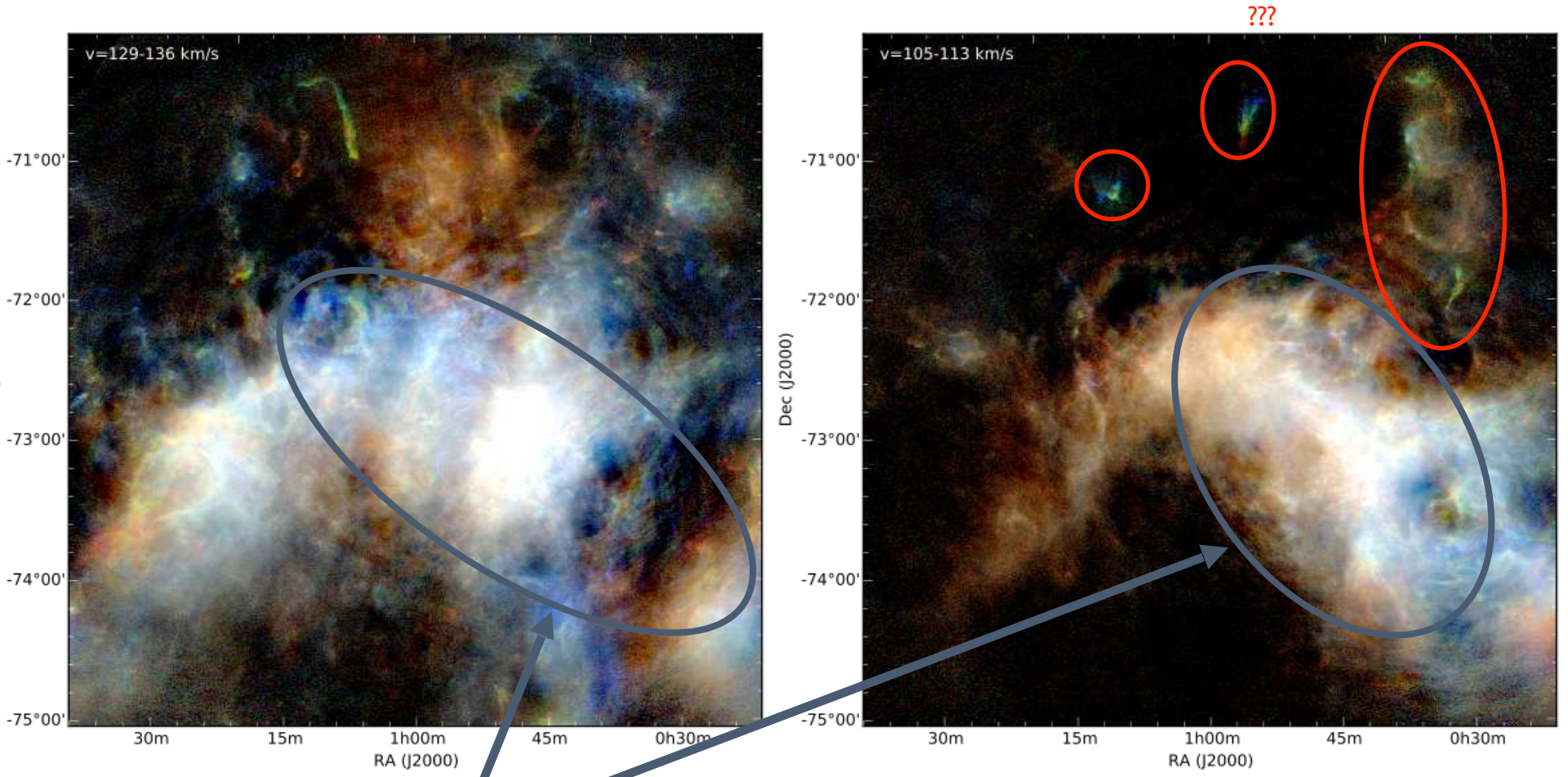

"Normally" rotating gas

Anomalous external features

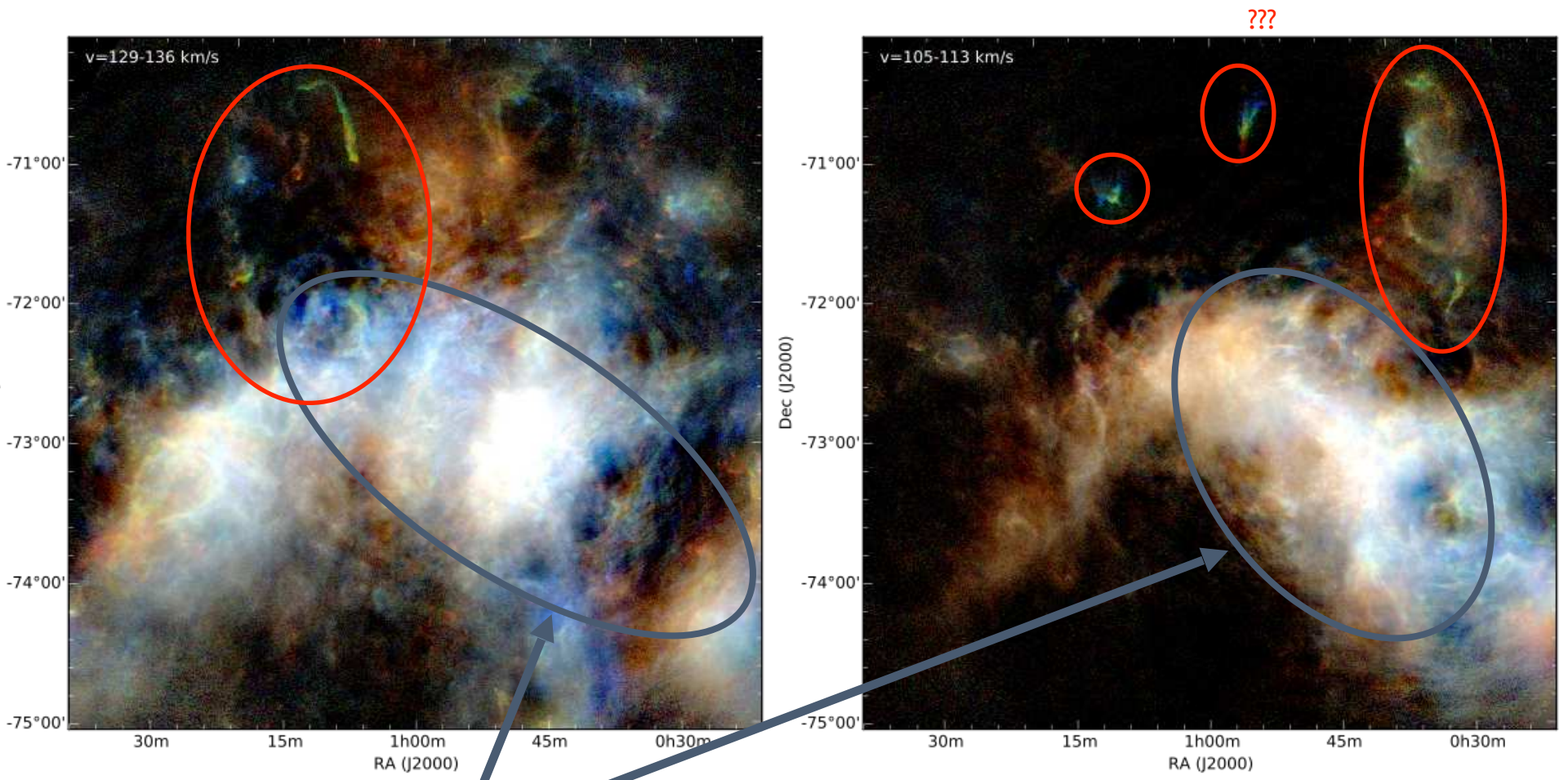

"Normally" rotating gas

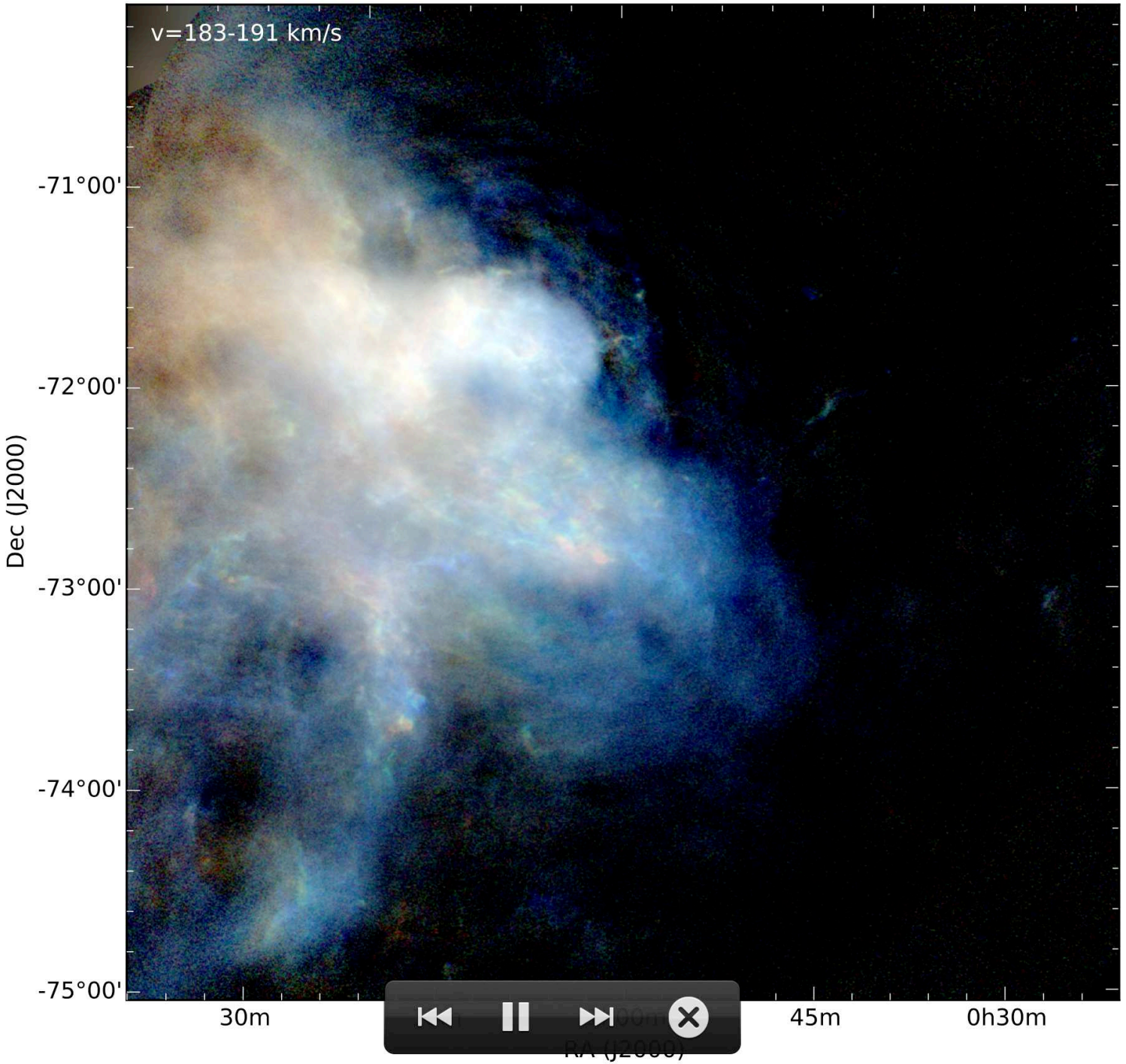
v=183-191 km/s
-71°00'
-72°00'
-73°00'
-74°00'
-75°00'
Dec (J2000)
30m
45m
0h30m
RA (J2000)

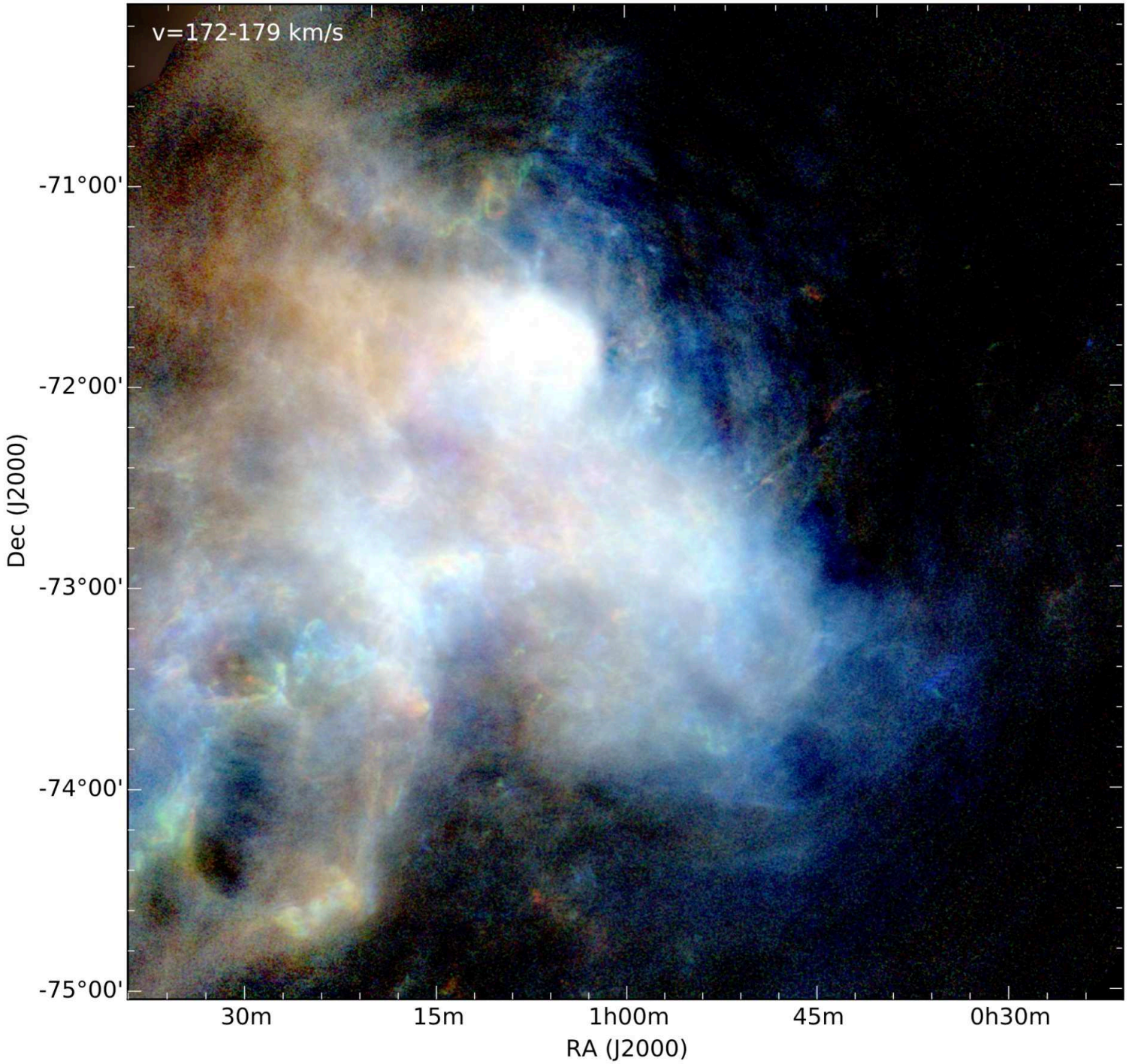
v=172-179 km/s
-71°00'
-72°00'
-73°00'
-74°00'
-75°00'
Dec (J2000)
30m
15m
1h00m
45m
0h30m
RA (J2000)

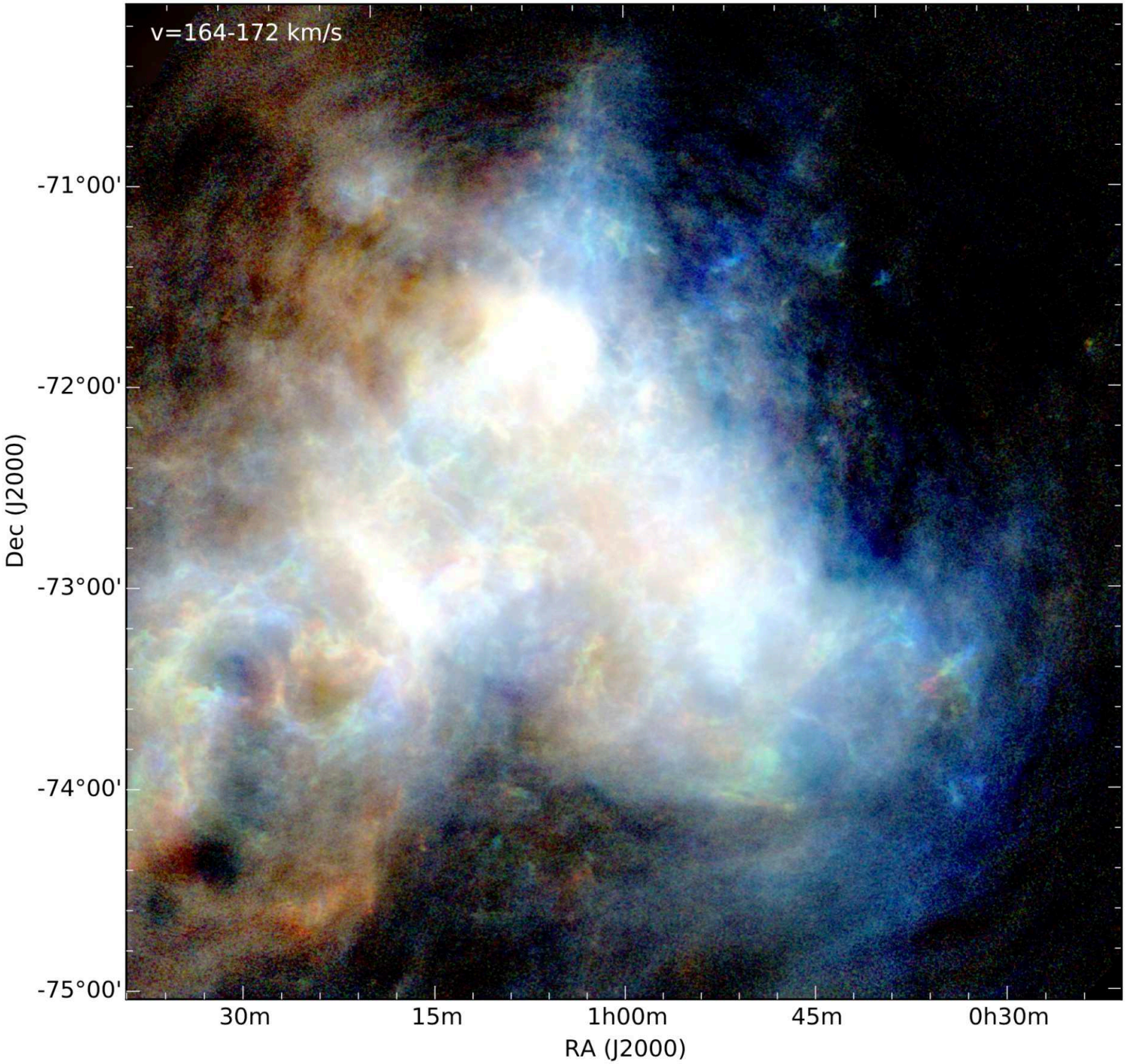
v=164-172 km/s
-71°00'
-72°00'
-73°00'
-74°00'
-75°00'
Dec (J2000)
30m
15m
1h00m
45m
0h30m
RA (J2000)

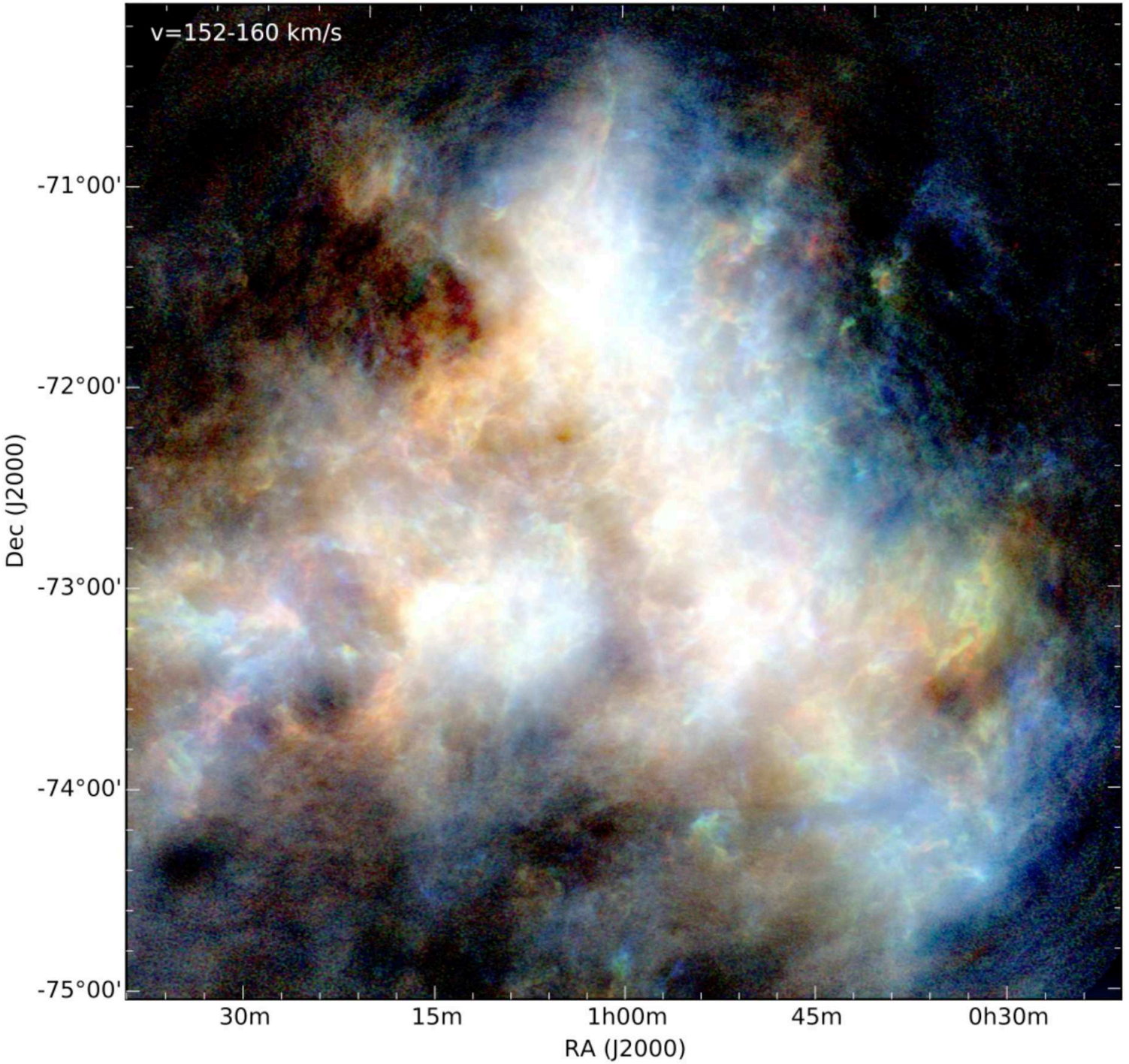
v=152-160 km/s
-71°00'
-72°00'
-73°00'
-74°00'
-75°00'
Dec (J2000)
30m
15m
1h00m
45m
0h30m
RA (J2000)

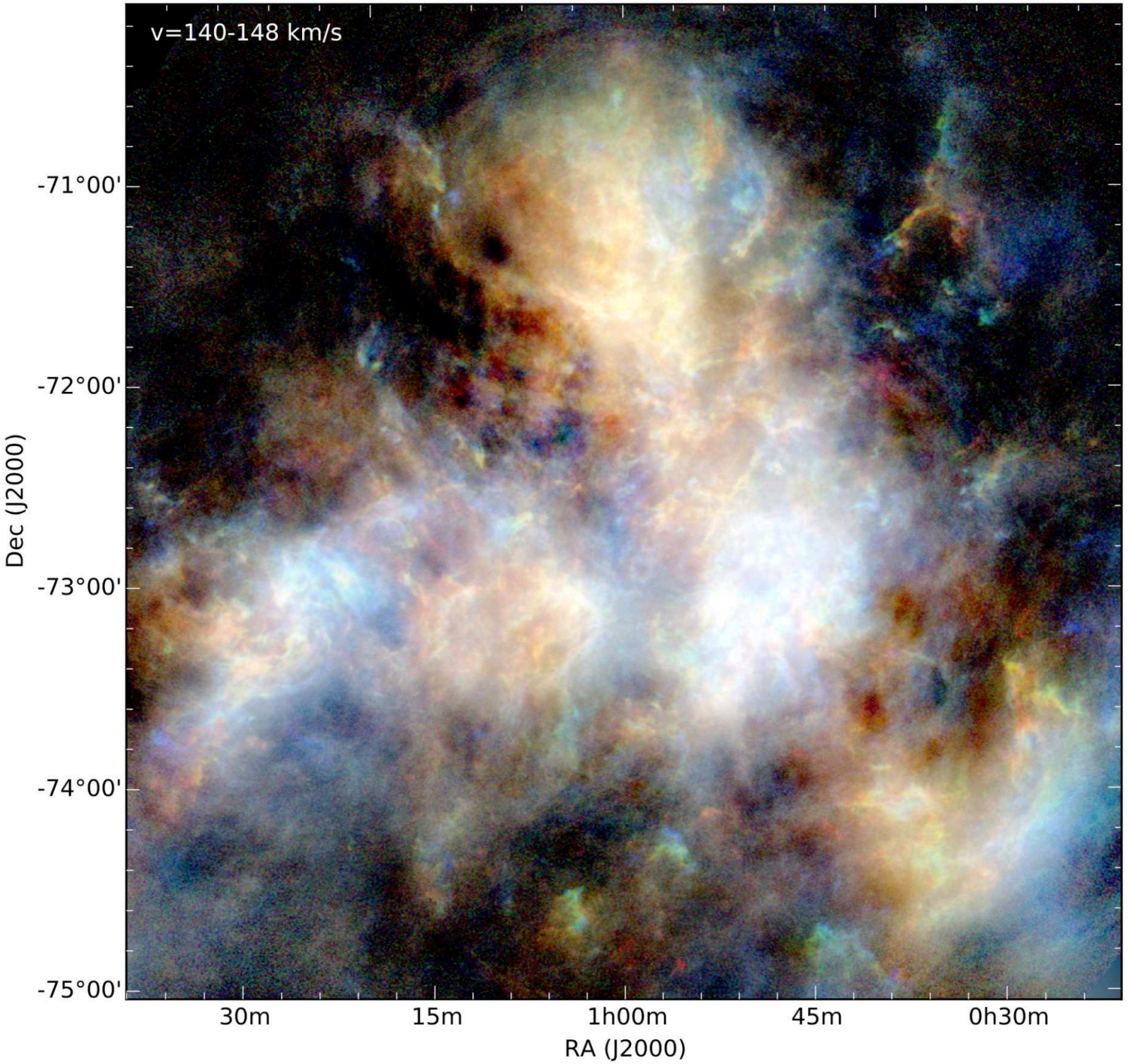
v=140-148 km/s
-71°00'
-72°00'
-73°00'
-74°00'
-75°00'
Dec (J2000)
30m
15m
1h00m
45m
0h30m
RA (J2000)

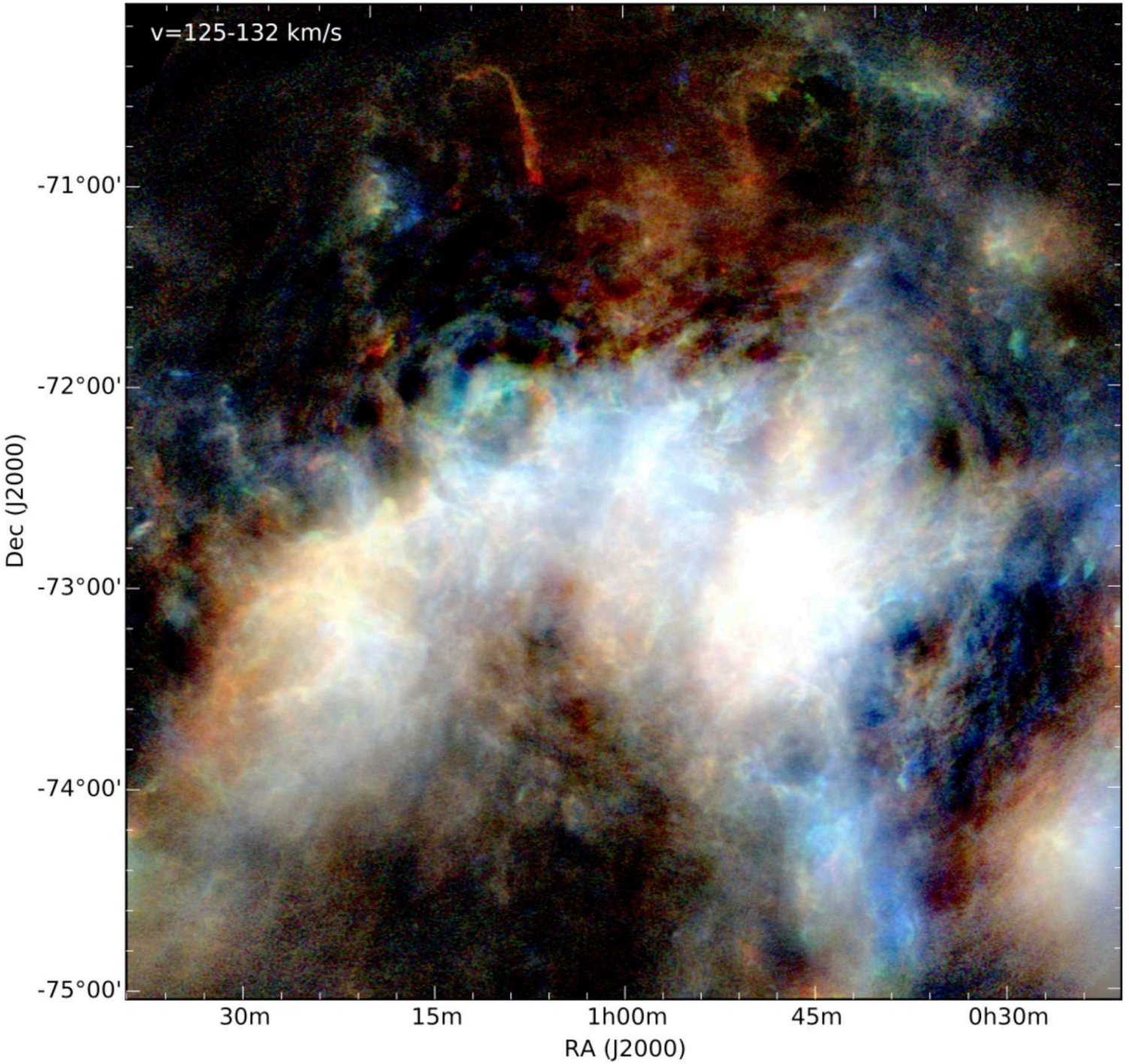
v=125-132 km/s
-71°00'
-72°00'
-73°00'
-74°00'
-75°00'
Dec (J2000)
30m
15m
1h00m
45m
0h30m
RA (J2000)

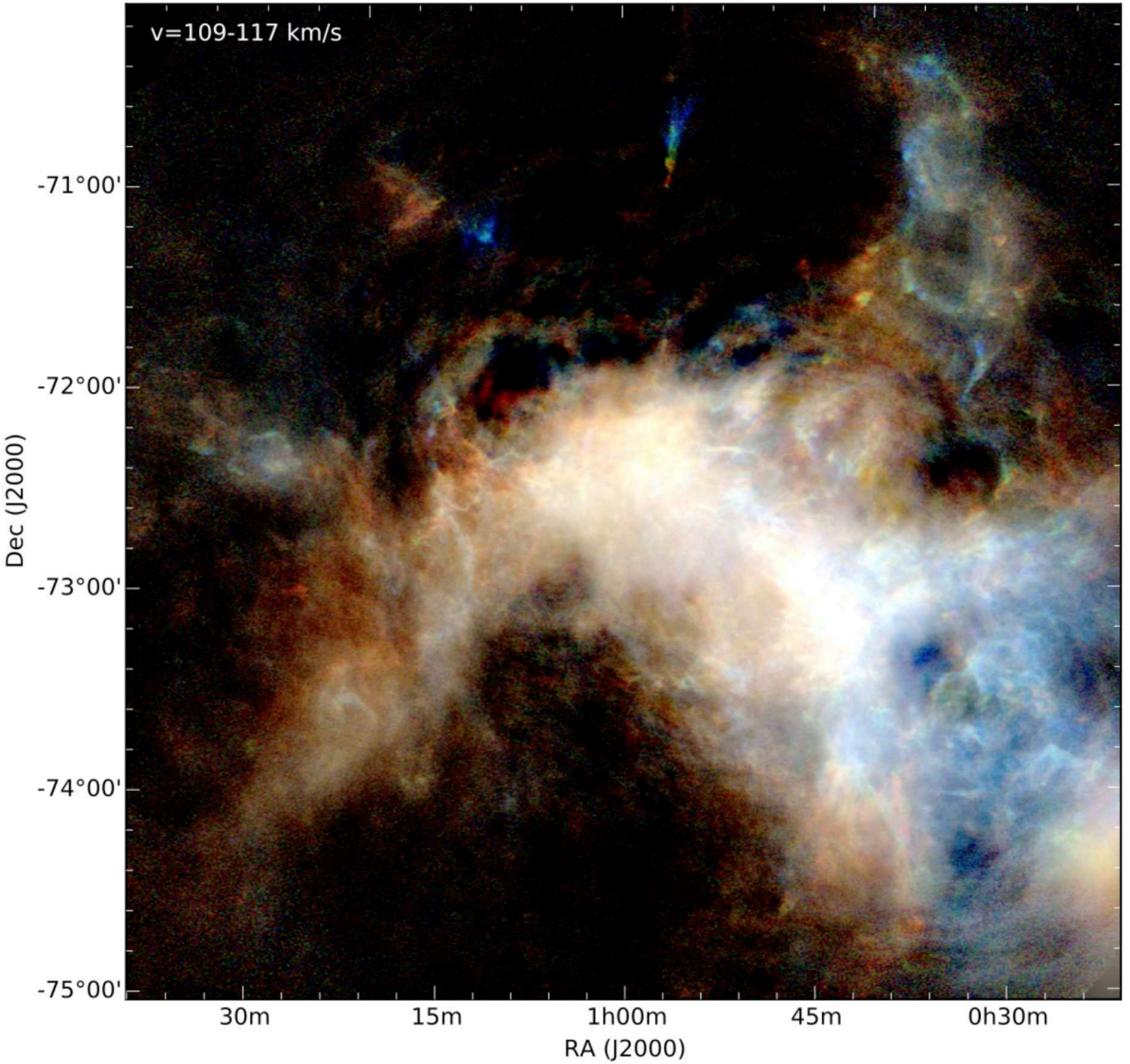
v=109-117 km/s
-71°00'
-72°00'
-73°00'
-74°00'
-75°00'
Dec (J2000)
30m
15m
1h00m
45m
0h30m
RA (J2000)

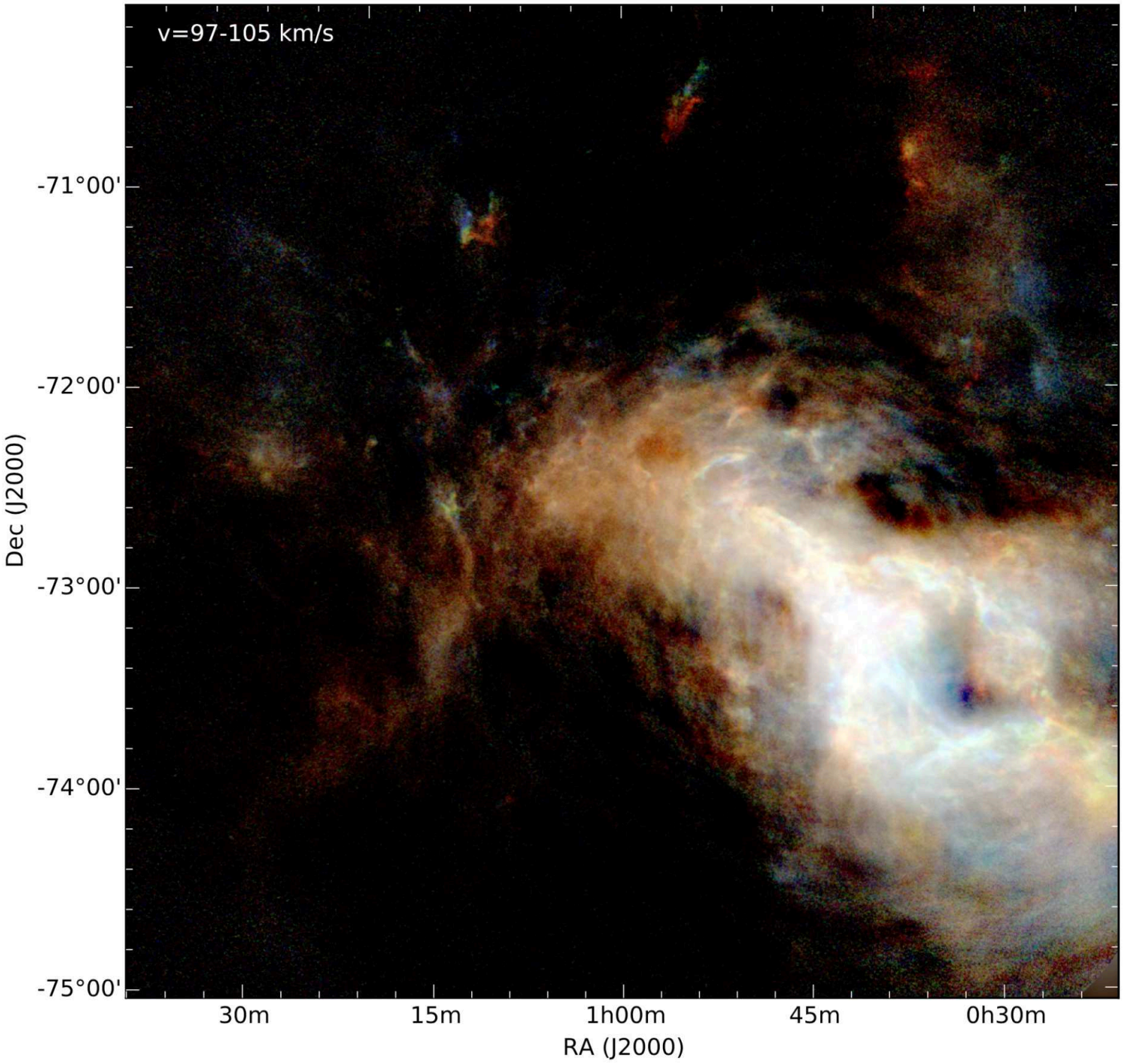
v=97-105 km/s
-71°00'
-72°00'
-73°00'
-74°00'
-75°00'
Dec (J2000)
30m
15m
1h00m
45m
0h30m
RA (J2000)

McClure-Griffiths et al. 2018 Nature-Astronomy in press.

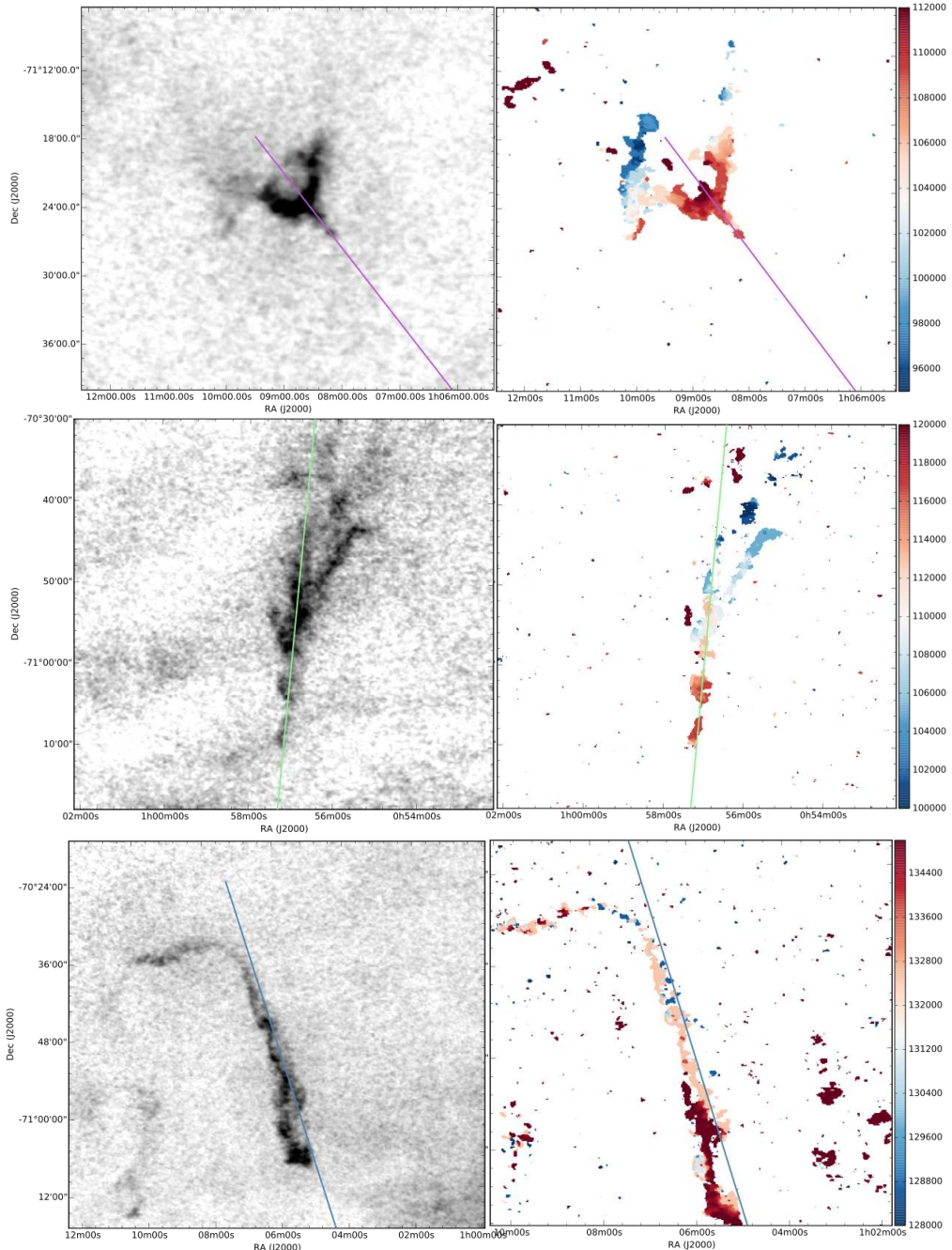

Filamentary features pointing back towards the bar

- Marginally resolved 10 -20 pc, 100 - 500 pc long
- Masses: 4.2 - 9.4 x10^4 $M_\odot$, most massive 2.2 x10^6 $M_\odot$
- Unresolved linewidths: T<400 K
- v_{dev} = 35 - 60 km/s

HI mass flux:

- M_{HI}~0.2 - 1 $M_\odot$ yr-1

Cool gas in the Magellanic System

Epoch 1: ATCA 21-cm Absorption studies of the Magellanic System with Parkes emission (Dickey et al. 1994, Mebold et al. 1997, Marx-Zimmer et al. 2000)

Epoch 2: Recent work with the ATCA:
Boyang Liu et al. (2018 in prep.)
Katie Jameson et al. (2018 in prep.)
and
Recent work with ASKAP:
McClure-Griffiths et al. (2018 in prep.)

Jameson et al. 2018 in prep.

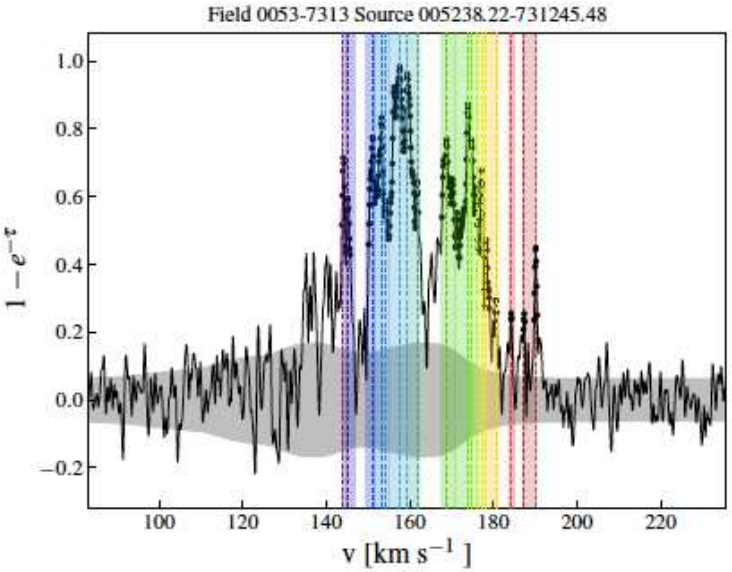

Figure 9. Absorption spectrum for source 005238.22-731245.48 with individual absorption features identified with different colors with the dashed line of the respective color indicating the absorption feature peak. The filled light gray area shows the variation of the emission spectra within one beam of the source location (same as Figure 3). The complete figure set (26 images) is available in the online journal.

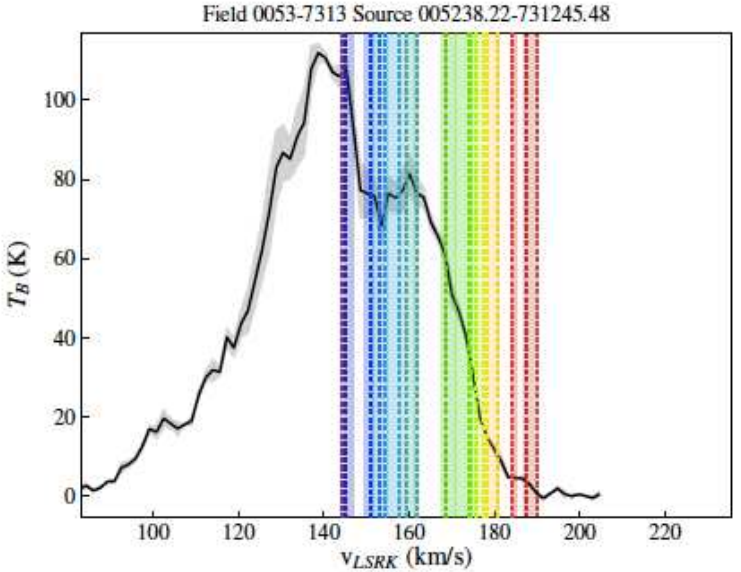

Figure 10. Emission spectrum for source 005238.22-731245.48 with individual absorption features identified with different colors with the dashed line of the respective color indicating the absorption feature peak (same as Figure 9). The filled gray area shows the 1σ uncertainty on the spectrum and the black points show the individual data points detected at $> 3\sigma$ that were used to identify features. The complete figure set (26 images) is available in the online journal.

HI Absorption vs. Emission

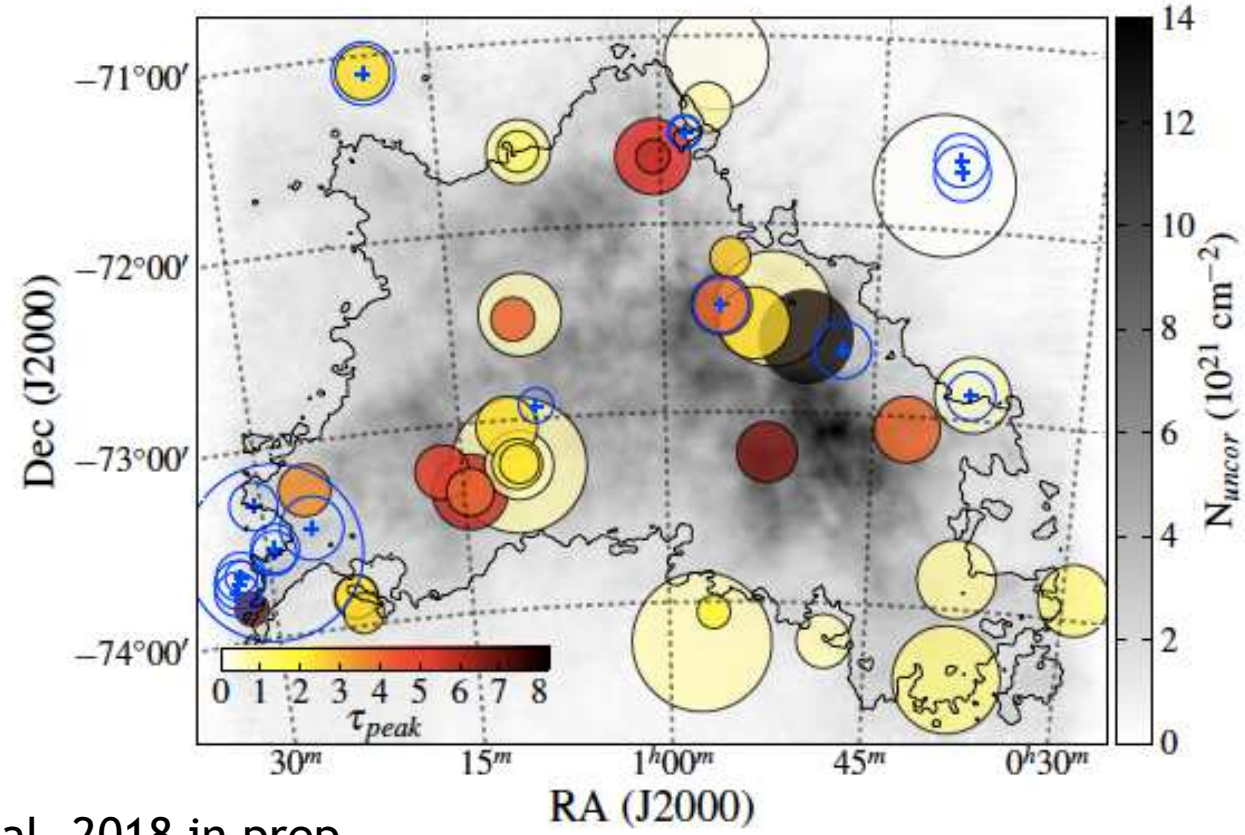

Jameson et al. 2018 in prep.

Figure 5. Map of the detected continuum sources with detected absorption ($\tau_{peak} > 3\sigma_\tau$) with the value of τ_{peak} shown with circle, sources with no detected absorption are shown with blue circles with crosses, and the column density of H I (assuming optically thin emission) shown in grayscale. The size of the circle indicates the relative strength of the continuum source. Most of the optically thick H I is located wihthin the main body of the galaxy, which indicated with the contour showing $N_{uncor} = 2 \times 10^{21}$ cm^{-2}.

Jameson et al. 2018 in prep.

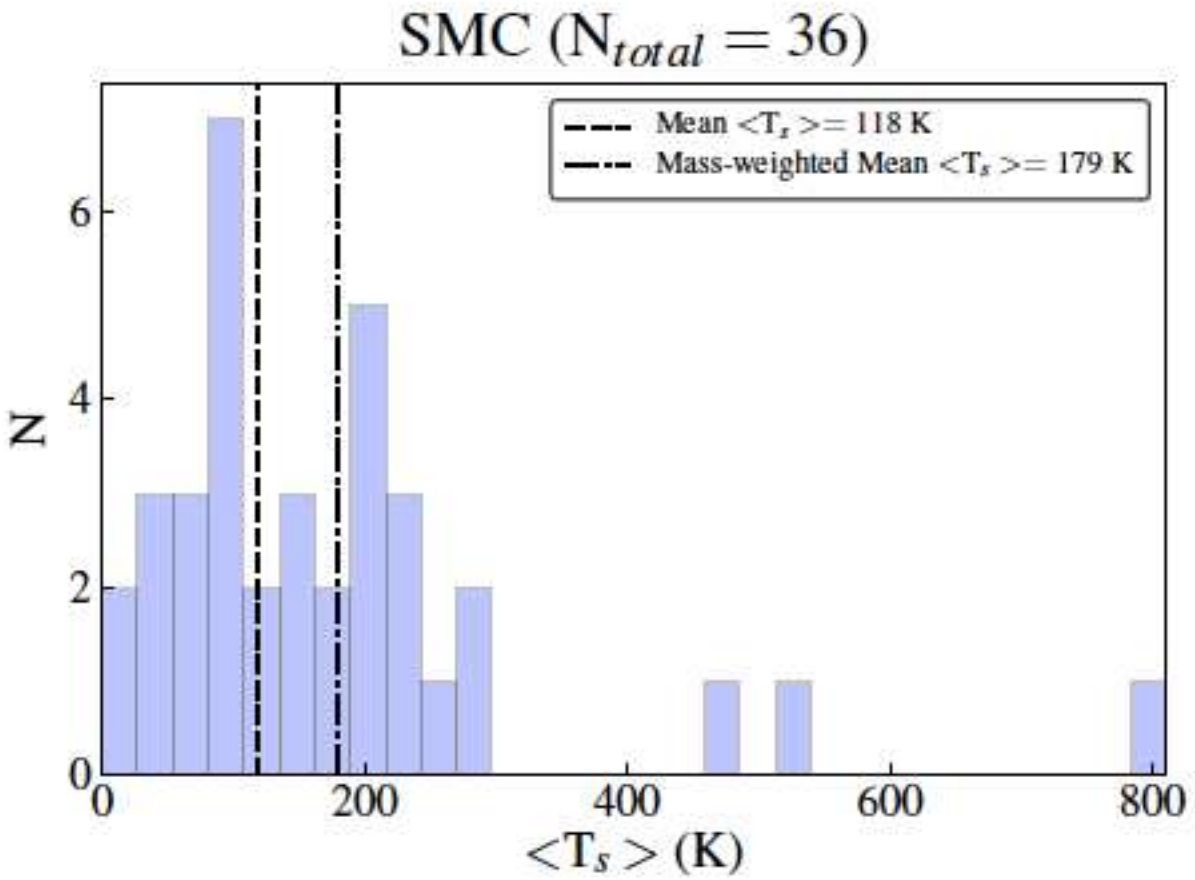

Figure 6. Histogram of the average H I spin temperature ($< T_s >$) that are detected at $> 3\sigma$ with the dashed line showing the mean of $< T_s > \sim$ 120 K and the dash-dot line showing the mass-weighted mean of $< T_s > \sim$ 180 K.

Conclusion:

- Improving the resolution and sensitivity in emission brings new astrophysical understanding of the relationship between star formation (SF) and outflow.
- Increasing the sample of absorption spectra shows where conditions are right for cool HI and eventual SF.
- Gas dynamics shows how the interaction between the MW halo and the MCs is changing the evolution of all three galaxies.

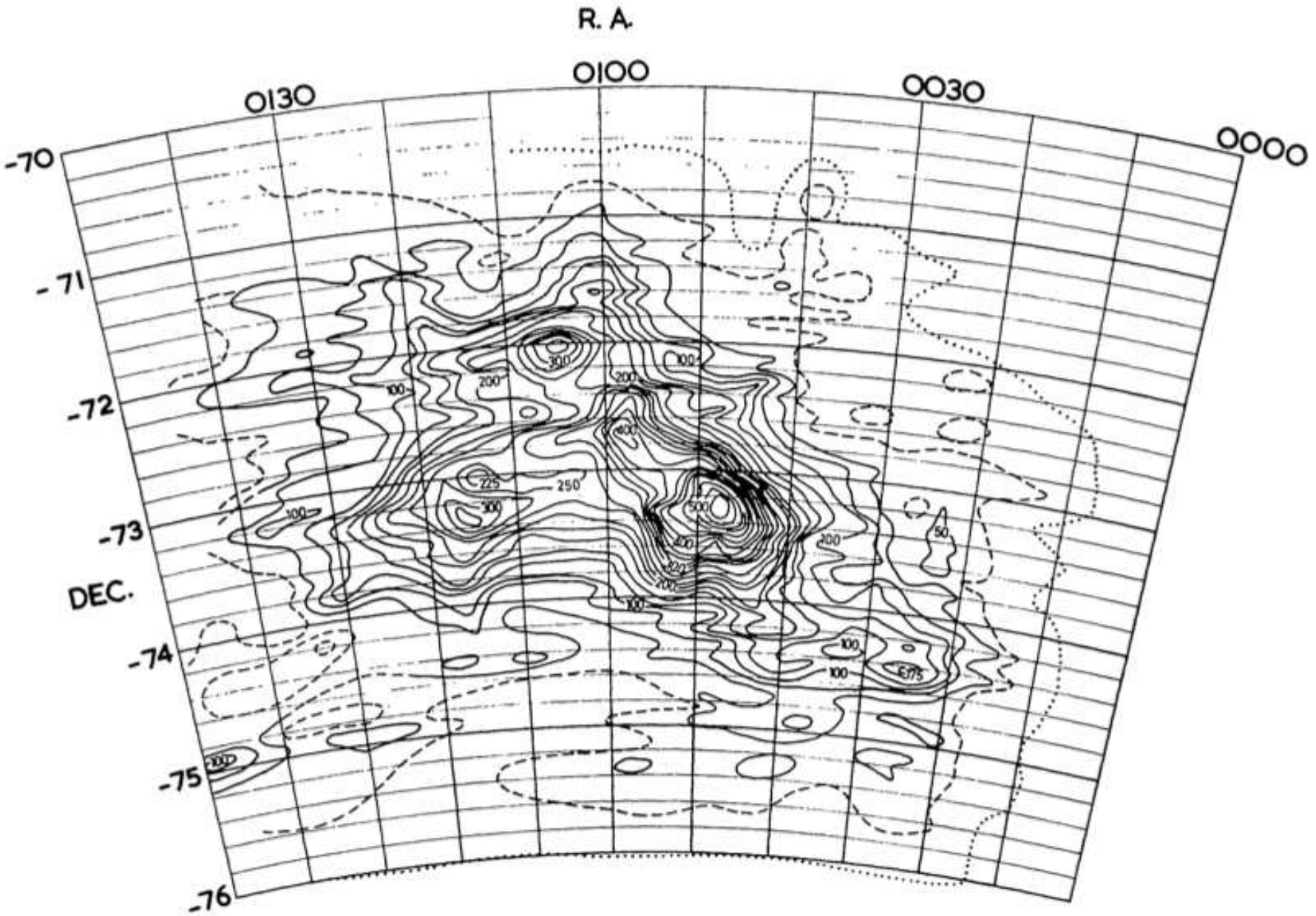

Fig. 2.—Contours of 21 cm H-line integrated brightness over the area of the SMC (contour unit = $3 \cdot 5 \times 10^{-17}$ W m^{-2} sr^{-1}). The outer (dotted) contour is an estimate of the limits of detectable radiation with the present receiver sensitivity. Epoch of coordinates 1975.

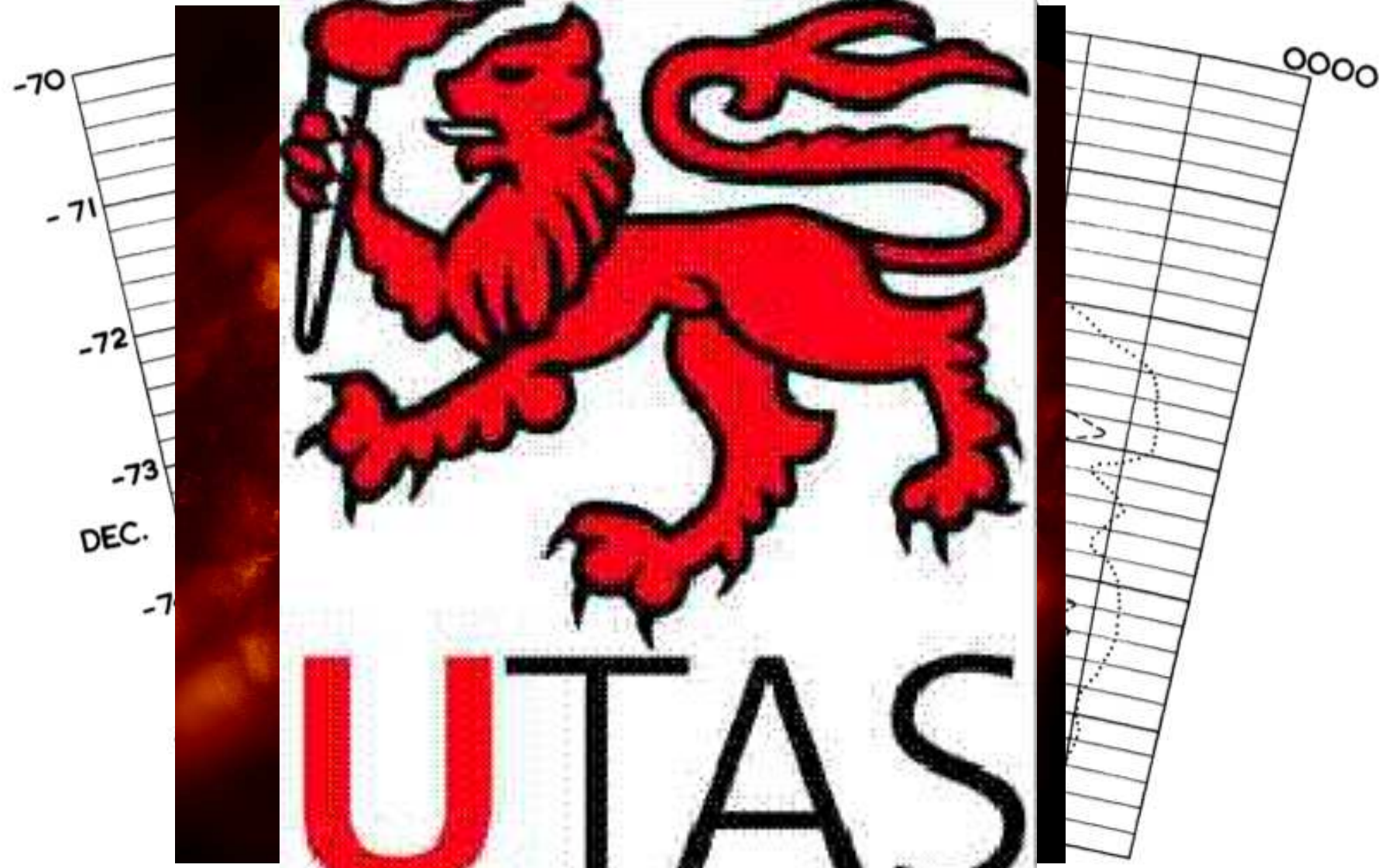

Figure 3. An H
H I column den

Fig. 2.—Cont he SMC (contour unit = $3 \cdot 5 \times 10^{-17}$ W m^{-2} sr^{-1}). The outer (dotted) contour is an estimate of the limits of detectable radiation with the present receiver sensitivity. Epoch of coordinates 1975.

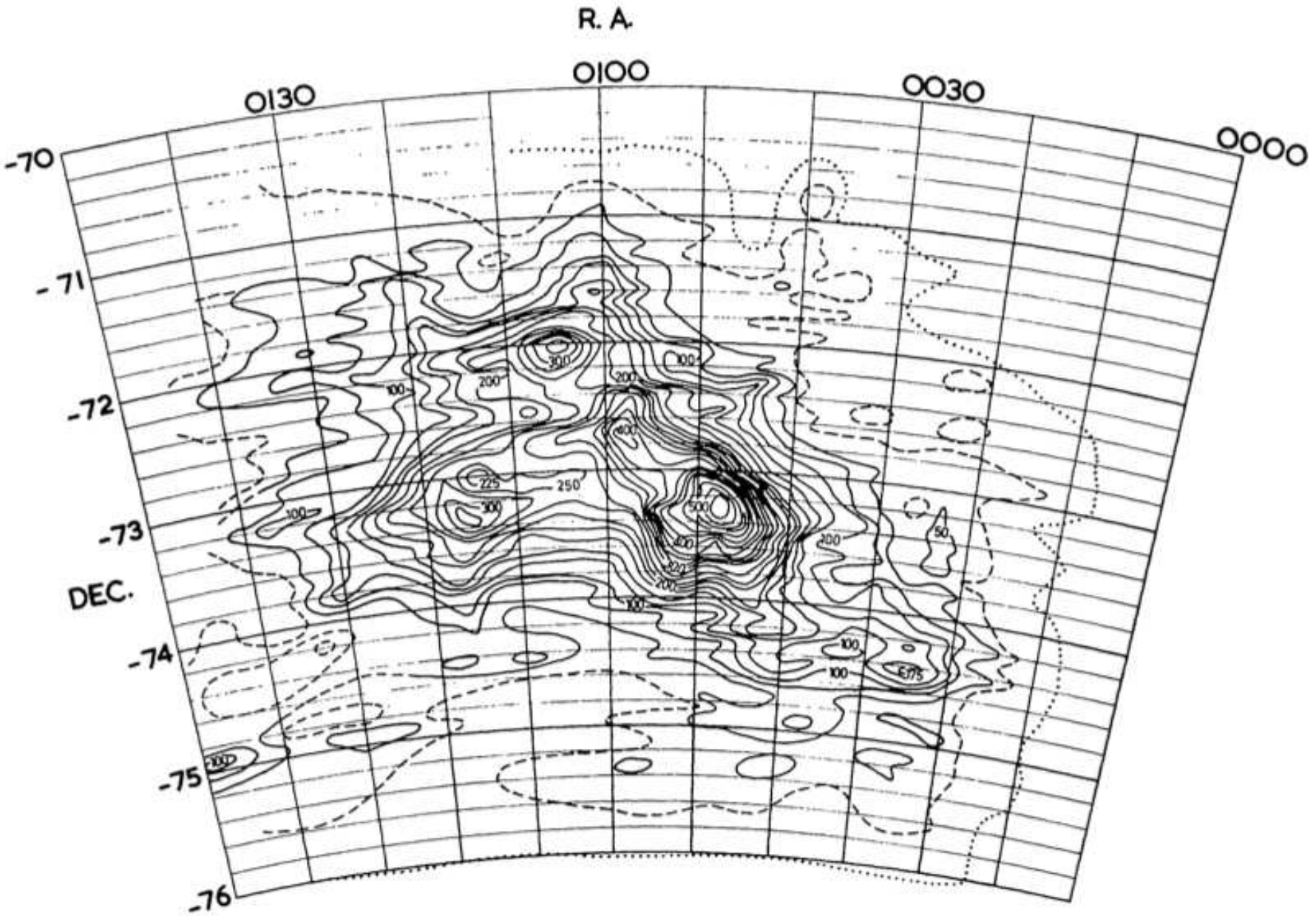

Fig. 2.—Contours of 21 cm H-line integrated brightness over the area of the SMC (contour unit = $3 \cdot 5 \times 10^{-17}$ W m^{-2} sr^{-1}). The outer (dotted) contour is an estimate of the limits of detectable radiation with the present receiver sensitivity. Epoch of coordinates 1975.

R. A.

-70

- 71

-72

-73

DEC.

0000

Figure 3. An H
H I column den

Fig. 2.—Cont he SMC (contour unit = $3 \cdot 5 \times 10^{-17}$ W m^{-2} sr^{-1}). The outer (dotted) contour is an estimate of the limits of detectable radiation with the present receiver sensitivity. Epoch of coordinates 1975.

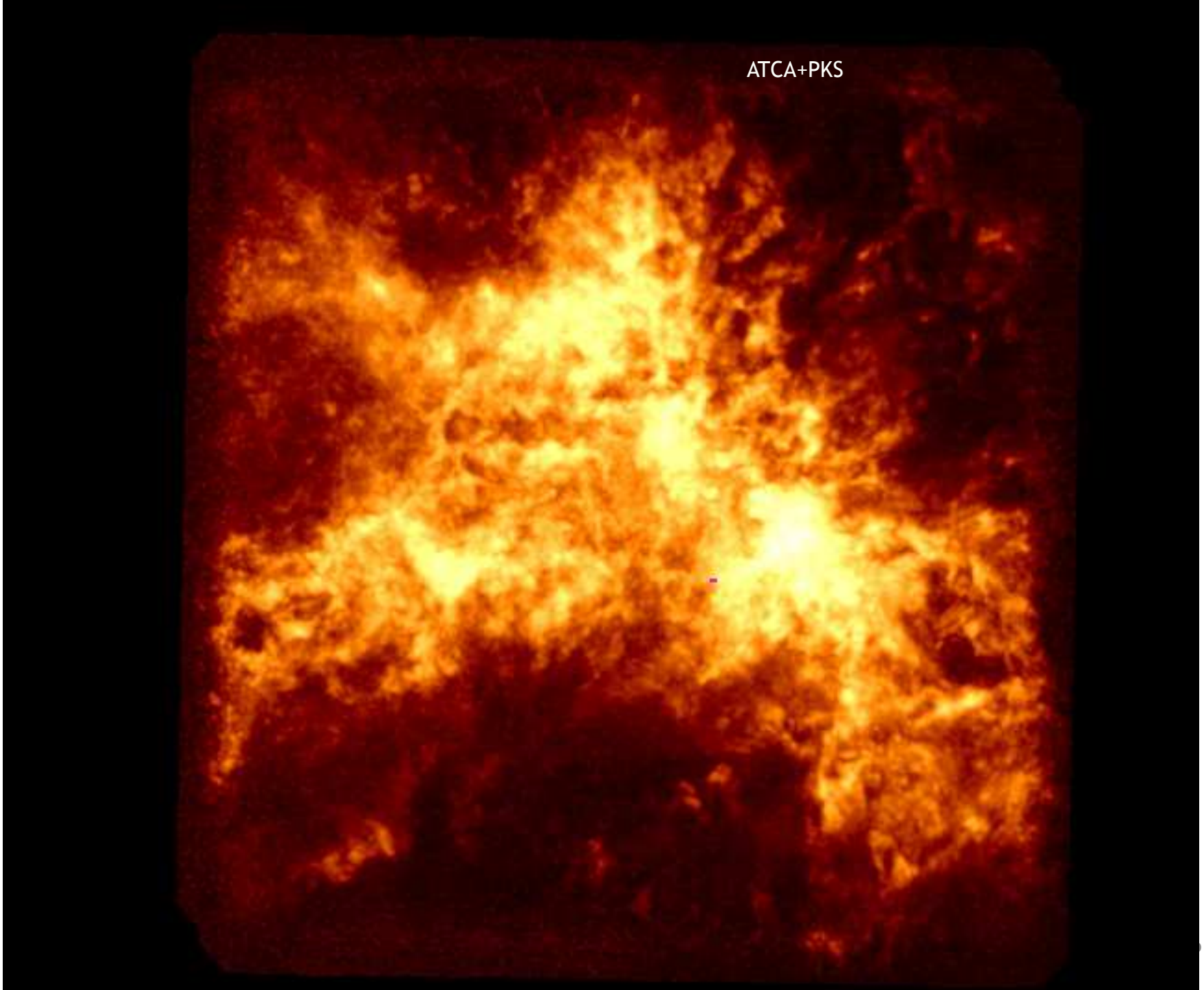
ATCA+PKS


ASKAP+Parkes
16 Antennas
McClure-Griffiths et al